Doctorate Program in Molecular Oncology and Endocrinology
Doctorate School in Molecular Medicine

XXVIII cycle - 2012–2015
Coordinator: Prof. Massimo Santoro

”Inhibition of Heat Shock Protein 27 (Hsp27) sensitizes Non-Small Cell Lung Cancer Cells to Epidermal Growth Factor Receptor (EGFR) inhibitors”

Dr. Lucia Nappi

University of Naples Federico II
Dipartimento di Medicina Clinica e Chirurgia

Administrative Location

Dipartimento di Medicina Molecolare e Biotecnologie Mediche
Università degli Studi di Napoli Federico II

Partner Institutions

- Università degli Studi di Napoli "Federico II", Naples, Italy
- Istituto di Endocrinologia ed Oncologia Sperimentale "G. Salvatore", CNR, Naples, Italy
- Seconda Università di Napoli, Naples, Italy
- Università degli Studi di Napoli "Parthenope", Naples, Italy

Faculty

Francesco Beguinot
Roberto Bianco
Bernadette Biondi
Francesca Carlomagno
Maria Domenica Castellone
Gabriella Castoria
Angela Celetti
Annamaria Cirafici
Annamaria Colao
Gerolama Condorelli
Valentina De Falco
Vittorio De Franciscis
Sabino De Placido
Gabriella De Vita
Monica Fedele
Pietro Formisano
Alfredo Fusco
Fabrizio Gentile
Domenico Grieco
Michele Grieco
Maddalena Illario
Paolo Laccetti
Antonio Leonardi
Paolo Emidio Macchia
Rosa Marina Melillo
Claudia Miele
Nunzia Montuori
Roberto Pacelli
Giuseppe Palumbo
Giovanna Maria Pierantoni
Rosario Pivonello
Giuseppe Portella
Maria Fiammetta Romano
Giuliana Salvatore
Massimo Santoro
Donatella Tramontano
Giancarlo Troncone
Giancarlo Vecchio
Mario Vitale

Inhibition of Heat Shock Protein 27 (Hsp27) sensitizes Non-Small Cell Lung Cancer Cells to Epidermal Growth Factor Receptor (EGFR) inhibitors

TABLE OF CONTENTS

LIST OF PUBLICATIONS

This dissertation is based upon the following publications:

1. Al Nakouzi N, Wang KC, Beraldi E, Jager W, **Nappi L**, Fazli L, Ettinger S, Bishop J, Zhang F, Chauchereau A, Loriot Y and Gleave M. Clusterin knockdown sensitizes prostate cancer cells to taxane by modulating mitosis. Submitted to EMBO Molecular Medicine.

2. **Nappi L**, Black P and Eigl B. Building the case for adjuvant chemotherapy after radical cystectomy. Accepted by Urology.

3. **Nappi L**, Gleave ME. PARP inhibition in castration-resistant prostate cancer. Future Oncol. 2016 Jan 21.

4. Barbara Lelj-Garolla, Masafumi Kumano, Eliana Beraldi, **Lucia Nappi**, Palma Rocchi, Diana N. Ionescu, Ladan Fazli, Amina Zoubeidi, and Martin E. Gleave
Hsp27 inhibition with OGX-427 sensitizes non-small cell lung cancer cells to erlotinib and chemotherapy. Mol Cancer Ther. 2015 May;14(5):1107-16.

5. Luigi Formisano#, **Lucia Nappi**#, Roberta Rosa, Roberta Marciano, Claudia D'Amato, Valentina D'Amato, Vincenzo Damiano, Lucia Raimondo, Francesca Iommelli, Antonella Scorziello, Giancarlo Troncone, Bianca Maria Veneziani, Sarah J Parsons, Sabino De Placido and Roberto Bianco.
Epidermal growth factor-receptor activation modulates Src-dependent resistance to lapatinib in breast cancer models. Breast Cancer Res. 2014 May 5;16(3):R45.

6. Claudia D'Amato, Roberta Rosa, Roberta Marciano, Valentina D'Amato, Luigi Formisano, **Lucia Nappi,** Lucia Raimondo, Concetta Di Mauro, Alberto Servetto, Marina Accardo, Chiara Carlomagno, Cataldo Bianco, Fortunato Ciardiello, Bianca Maria Veneziani, Sabino De Placido and Roberto Bianco.

Inhibition of Hedgehog signaling by NVP-LDE225 (Erismodegib) interferes with growth and invasion of human renal cell carcinoma cells. Br J Cancer. 2014 Sep 9;111(6):1168-79.

7. Valentina D'Amato, Roberta Rosa, Claudia D'Amato, Luigi Formisano, **Lucia Nappi**, Roberta Marciano, Lucia Raimondo, Concetta Di Mauro, Alberto Servetto, Celeste Fusciello, Bianca Maria Veneziani, Sabino De Placido and Roberto Bianco
The dual PI3K/mTOR inhibitor PKI-587 enhances sensitivity to the anti-EGFR monoclonal antibody cetuximab in human head and neck cancer models. Br J Cancer. 2014 Jun 10;110(12):2887-95.

8. Roberta Rosa, Roberta Marciano, Luigi Formisano, **Lucia Nappi**, Claudia D'Amato, Vincenzo Damiano, Gabriella Marfè, Silvana Del Vecchio, Antonella Zannetti, Adelaide Greco, Umberto Malapelle, Giancarlo Troncone, Alfonso De Stefano, Chiara Carlomagno, Bianca Maria Veneziani, Sabino De Placido, Roberto Bianco. Sphingosine Kinase 1 (SPHK1) overexpression contributes to cetuximab resistance in human colorectal cancer models. Clinical Cancer Research 2013 Jan 1;19(1):138-47.

9. Roberta Rosa, Vincenzo Damiano, **Lucia Nappi**, Luigi Formisano, Francesco Massari, Aldo Scarpa, Guido Martignoni, Roberto Bianco, Giampaolo Tortora. Angiogenic and signalling proteins affect resistance and choice of second line treatment in renal cell cancer. Br J Cancer. 2013 Aug 6;109(3):686-93.

10. Damiano V, Rosa R, Formisano L, **Nappi L**, Gelardi T, Marciano R, Cozzolino I, Troncone G, Agrawal S, Veneziani BM, De Placido S, Bianco R, Tortora G. Toll-like receptor 9 agonist IMO cooperates with everolimus in renal cell carcinoma by interfering with tumour growth and angiogenesis. Br J Cancer. 2013 Apr 30;108(8):1616-23.

11. Monteleone F, Rosa R, Vitale M, D'Ambrosio C, Succoio M, Formisano L, **Nappi L**, Romano MF, Scaloni A, Tortora G, Bianco R, Zambrano N.
Increased anaerobic metabolism is a distinctive signature in a colorectal cancer cellular model of resistance to antiepidermal growth factor receptor antibody. Proteomics. 2013 Mar;13(5):866-77.

ABSTRACT

Non-small cell lung cancer (NSCLC) is the most frequent cause of death from cancer worldwide. Despite the availability of active chemotherapy regimens and epidermal growth factor receptor (EGFR) tyrosine kinase inhibitors, all advanced patients develop recurrent disease after first-line therapy. While heat shock protein 27 (Hsp27) is a stress-induced chaperone that promotes acquired resistance in several cancers, its relationship to treatment resistance in NSCLC has not been defined. Understanding adaptive responses of acquired resistance will help guide new strategies to control NSCLC.

Hsp27 levels were evaluated in an HCC827 erlotinib-resistant derived cell line (HCC-827$_{Resistant}$), and sensitivity to erlotinib was examined in Hsp27 over-expressing A549 cells. The role of Hsp27 in both erlotinib and cytotoxic treatment resistance was evaluated in HCC827 and A549 NSCLC cells using the Hsp27 antisense drug OGX-427 and VPC-27, a new functional small molecule inhibitor of Hsp27. The effect of Hsp27 inhibitors in combination with erlotinib was also assessed in mice bearing A549 or HCC827 xenografts.

Hsp27 is induced by erlotinib and protects NSCLC cells from treatment-induced apoptosis, while Hsp27 inhibition sensitizes NSCLC cells to erlotinib. Interestingly, increased resistance to erlotinib was observed when Hsp27 was increased either in HCC827 ER or over-expressing A549 cells. Combining OGX-427 or VPC-27 with erlotinib significantly enhanced antitumor effects *in vitro* and delayed NSCLC cells growth *in vivo*.

These data indicate that treatment-induced Hsp27 (by inhibition of EGFR) contributes to the development of resistance, and provides pre-clinical proof-of-principle that inhibition of stress adaptive pathways mediated by Hsp27 enhances the activity of erlotinib in NSCLC.

INTRODUCTION

1. Non-Small Cell Lung Cancer

Lung cancer is the most prevalent cancer and the leading cause of cancer related death worldwide [1]. In North America and Europe it is the third most common cause of mortality for men and women and is increasingly observed in non-smokers. Non-small cell lung cancer (NSCLC), with a five-year rate survival of only 15%, accounts for approximately 80% of all lung cancers. NSCLC is classified histologically in: adenocarcinoma, squamous cell carcinoma and large cell carcinoma. The majority of patients present with either locally advanced disease (stage III) or metastatic disease (stage IV). Importantly, patients who undergo curative surgical resection for apparent localized disease have 50-80% survival rates implying the need for better systemic treatment to cure micro-metastatic disease [2]. Therefore, the majority of patients require systemic therapy. Several new drugs have been approved for the treatment of metastatic adenocarcinoma of the lung: bevacizumab, a monoclonal antibody against VEGF, is approved in combination with platinum and paclitaxel [3], nivolumab and pembrolizumab are anti-PD-1 agents, recently approved in second line in advanced non-squamous lung cancer [4-5]. Ramucimurab is a VEGFR-2 monoclonal antibody approved as second line therapy in combination with docetaxel after chemotherapy failure [6]. For patients with adenocarcinoma harboring ALK mutations, crizotinib represents the drug of choice [7]. Unfortunately, platinum-based doublet with gemcitabine remains the mainstay of front-line therapy for advanced squamous cell carcinoma with modest improvement in survival and quality of life [8].

2. Epidermal Growth Factor Receptor

Epidermal Growth Factor Receptor (EGFR) is a 170 KDa transmembrane tyrosine kinase receptor constitutively activated, either by over-expression or by mutation, in many solid tumors [9]. Its overexpression correlates with poor prognosis and resistance to conventional antitumor therapies [10]. The EGF receptor structure includes a N-terminal extracellular (EC) domain that recognizes and dimerizes with itself and with other receptors like HER-2, HER-3 and HER-4. EGF, Amphiregulin, Epiregulin, β-cellulin and TGF-α bind and activate the EC domain of EGFR [11]. In normal physiology both homodimerization and heterodimerization of EGFR are observed but heterodimerization with other activated receptors is more potent for the activation

of downstream signals [12]. The N-terminus is followed by a transmembrane portion and the C-terminal intracytoplasmic region that contains an ATP-dependent tyrosine kinase (TK) domain. This TK domain is able to autophosphorylate at tyrosine residues Y992, Y1045, Y1068, Y1086, S1142, Y1148, and Y1173 [13]. EGFR phosphoactivation regulates cell proliferation, survival, angiogenesis and metastasis via activation of several down-stream pathways, including mitogen-activated protein kinase (MAPK) and the phosphoinositide 3-kinase (PI3K)/AKT pathway [14]. EGFR activation is triggered by hetero-dimerization with other transmembrane receptors, most notably HER-3 and HER-2 [15]. However, in NSCLC mutations in the TK domain represent the main mechanism of activation of EGFR. These mutations create a conformational change in the intracytoplasmic region that leads to a constitutively phosphorylation of EGFR, completely independent from the ligands-mediated activation of the receptor [16]. Since it represents one of the most important drivers of NSCLC growth and survival, several drugs have been developed targeting EGFR. Cetuximab and panitumumab are recombinant monoclonal antibodies that recognize the EC portion of EGFR [17]. Erlotinib and gefitinib are small molecule EGFR inhibitors that binds the ATP-binding site of the intracellular TK domain of EGFR [18]. Afatinib is a new generation irreversible EGFR-TKI that affects both EGFR and HER-2 [19]. Afatinib, erlotinib and gefitinib significantly improve survival in patients with metastatic NSCLC and are approved for the first line therapy of patients with metastatic adenocarcinoma of the lung harboring EGFR activating mutations [20-23]. Although the development of EGFR targeting drugs have modified the clinical landscape for patients with metastatic NSCLC, unfortunately therapeutic resistance and death from disease remains very common. Resistance is often associated with the development of second EGFR mutations (i.e. T790M,) that interfere with binding to the inhibitors to maintain EGFR activity [24], which can be partially overcome by increasing TKI potency [25] or by co-targeting other pathways up-regulated during treatment. For example, there is evidence that co-targeting Heat shock protein 90 (Hsp90), a molecular chaperone known to interact with EGFR, can increase EGFR molecular degradation even in the presence of mutations [26]. Other heat shock chaperones, like Hsp27 (HspB1), play a pivotal role in stress responses to treatment, but their role has not been investigated in the resistance to EGFR inhibitors in NSCLC. Better understanding the mechanisms of resistance to anti EGFR drugs is necessary to re-sensitize cancer cells and continue to improve outcomes, and to better stratify and predict treatment response to control resistance.

3. Heat Shock Protein 27 (Hsp27)

Hsp27 is a stress-induced ATP-independent molecular chaperone that is transcriptionally regulated by HSF-1, HIF-1α, and other factors influenced by cell type and cell context [27-28]. It is involved in the regulation of protein homeostasis, in stabilizing unfolding proteins, as well as the actin-cytoskeleton [29-31]. Hsp27 promotes survival by binding to both cytochrome *c* and caspase 3 to inhibit intrinsic apoptotic pathway activation, and facilitates epithelial-mesenchymal transition and expression of metastatic genes [32-33]. Its activity is regulated by phosphorylation that controls Hsp27 oligomerization and self-association [34]. In prostate cancer (Pca), Hsp27 controls treatment resistance facilitating cell survival, invasion and migration [33, 35-36]. Hsp27 expression increases after androgen deprivation therapy (ADT) and it is highly expressed in castration resistant prostate cancer, activating alternative molecular pathways (AR, IGF-1, and IL-6) that support cell proliferation and survival independently from castration [37-39]. Moreover, Hsp27 is also involved in the control of endoplasmic reticular (ER) stress [40]. These data support Hsp27 as a therapeutic "hyper-node", a target situated as a 'Hub" at the center of many pathways, regulating response of cells to therapeutic stress and contributing to the development of therapy resistance.

4. Targeting Hsp27

Hsp27 is a difficult protein to target because, unlike Hsp90, it lacks an active site or ATP-binding pocket. The Anti Sense Oligonucleotide (ASO) OGX-427 is the only Hsp27 inhibitor that showed to efficiently block Hsp27 functions in preclinical models of prostate cancer [41]. It was developed by Dr. Gleave's group at the Vancouver Prostate Centre and demonstrated high anti-cancer activity *in vitro* and *in vivo* prostate cancer models [33, 42]. The stability of the drug was significantly improved by the presence of a 2′-methoxyethyl phosphorothioate group that reduce the nucleases degradation improving the in vivo tissue half-life of the drug (almost 7 day). Hsp27 ASO enhances apoptosis and delays prostate tumor progression and chemo-sensitizes bladder, prostate, ovarian and uterine cancer to paclitaxel [43-44], and colorectal cancer to irinotecan [45]. Considering the promising activity of the drug, a phase I clinical trials with OGX-427, alone or in combination with docetaxel, was conducted in patients affected by prostate, bladder, breast and lung cancer. The study demonstrated that OGX-427 was well

tolerated at high doses (800 and 1000 mg) also in combination with docetaxel [46]. A recent phase II trial investigating OGX-427 with or without prednisone (P) on progression in chemo-naive metastatic CRPC enrolled 72 patients. At 12 weeks, the proportion of patients that were progression free was 71% in OGX-427+P arm and 40% in P only arm. A ≥50% PSA decline occurred in 50% of patients on OGX-427+P compared to 20% on P. Measurable disease response occurred in 44% on OGX-427+P and 0 patients on P. Circulating Tumor Cells conversion from ≥5 to <5/7.5 ml blood occurred in 55% evaluable patients on OGX-427+P and 41% treated with P. These results confirm, for the first time, single agent activity for an Hsp27 inhibitor in cancer, supporting the central role of Hsp27 in the development of prostate cancer [47]. OGX-427 also showed activity in a phase I trial in superficial bladder cancer, inducing 38% of complete pathologic response. These results confirm, for the first time, single agent activity for an Hsp27 inhibitor [48]. However, while the clinical results of OGX-427 are promising, a more potent and orally active inhibitor, with higher stability, may improve cancer outcome.

So far, no small molecules have showed to efficiently inhibit Hsp-27. Because of the lack of an ATP binding domain and its extremely dynamic structure [49], targeting Hsp27 is challenging. Most sHsps assemble into large oligomers which stably interact with misfolded or other specific client proteins, facilitating proteostasis along with signaling and transcriptional pathways activation. Depending on the number of subunits, these Hsp27 oligomers have diverse architectures and symmetries that determine the spectrum of their highly context-dependent protein interactome. Assembly and depolymerisation of Hsp27 subunits into large to small complexes is dynamic and context dependent, mediated by the phosphorylation status of 3 serine residues (Ser15, Ser78, Ser82) in the N-terminal region of Hsp27 [50-51]. Thus, the N-terminal domain modulates dynamics of Hsp27 oligomer assembly and is critical for the affinity of Hsp27 with client proteins.

In this study we show that Hsp27 is expressed in nearly 70-80% of NSCLC patients and that erlotinib increases levels of both total and phosphorylated Hsp27 via activation of HSF-1. Using Hsp27 functional biochemical screening assays, we identified a new small molecule drug, VPC-27, that inhibits Hsp27 phosphor-activation after treatment stress in several cancer cells with a good tolerability profile in mice studies.

Hsp27 inhibition with OGX-427 or the new small molecule Hsp27 inhibitor VPC-27 synergistically increased erlotinib-induced apoptosis and inhibition of A549 and HCC827 lung

cancer cell growth *in vitro* and *in vivo*. These results illustrate that co-targeting treatment-induced adaptive responses mediated by Hsp27 can sensitize lung cancer cells to EGFR TKIs and cytotoxic therapies.

MATERIALS AND METHODS

FRET

Fluorescence Resonance Electricity Transmission (FRET) assay was performed in Corning 384 wells, black flat bottom plates. 20µL of Buffer (10mM Tris pH 8.4), 5µL Inhibitor (200µM), 10µL Rodamine Red:Hsp27 (45nM), 10µL QSY21:Hsp27 (0.675µL) was successively added to sample wells. Samples were incubated for 20minutes at 37°C prior to fluorescence measurements using TECAN INFINITE M200PRO, excitation wavelength of 515nm and emission wavelength of 590nm.

FP

After FRET measurements, 10µL of wt-Hsp27 (2.475µM), 10µL of Insulin-FITC (1.56µM) and 10µM TCEP (75mM) was added to appropriate wells with 2 minute equilibration period in between each addition. The plate was then incubated at 42°C for 20 minutes and Fluorescence Polarization (FP) measurements were taken (TECAN INFINITE F500 excitation wavelength 485nM and emission wavelength at 535nM).

Aggregation

HSF1 -/- MEF cells were lysed using 25mM Tris pH7.4, 150mM NaCl, 1mM EDTA, 1% NP40 lysis buffer. BSA 100g/L and 1M DTT was prepared in advance and was thawed at room temperature. Using Corning 96well plate, in each sample wells, 20µL of BSA, 100µL of cell lysates at 1mg/mL, 1µL of DMSO/test inhibitor, and ±1µL of 1mg/mL wt-Hsp27 successively added, PBS was used to complete to total volume of 320µL. After 5 minutes incubation at room temperature, the plate was subjected to 3-hour kinetic cycle with reading at 340nM at 42°C, shaken for 10 seconds prior to read, and was read every 5 minutes.

Oligomerization

A 12 steps glycerol gradient ranging from 3.33% to 40% was constructed with 3.33% stepwise increments with total volume of 9mL. Cell lysates were prepared in 25mM HEPES pH 7.4, 1mM EDTA, 3.33% Glycerol, 0.1mM PMSF, 1mM DTT and sonicated for 10 seconds. Equal amount of proteins, measured by BCA analysis, were loaded onto the glycerol gradient and subjected to ultracentrifugation for 18hours at 36 000RPM (160 000 x G) using SW41Ti swing bucket rotor. Three-hundred μL fractions were collected into corning 96well plates using a mini pump and stored at -30°C for WB analysis. Glycerol gradient assay buffer (25mM HEPES pH 7.4, 1mM EDTA, 1mM DTT) was used to make the glycerol gradients.

Tumor Tissue Arrays

Six hundred nine cases of primary NSCLCs with follow-up data diagnosed between 1978 and 2002 were identified from the archives of St Paul's Hospital, Vancouver, British Columbia. The paraffin-embedded tissue blocks were used to construct a duplicate core Tissue microarray (TMA). After review of the tissue cores, 588 cases, consisting of NSCLC met the criteria for inclusion in this study. Carcinoids, atypical carcinoids, large cell neuroendocrine carcinoma and metastatic tumors were all excluded. H&E-stained sections were reviewed and sub-classified as follows: 243 adenocarcinoma (AD), 272 squamous cell carcinoma (SCC), 35 large cell carcinoma (LCC), 32 non-small cell carcinoma, and 6 other (carcinoma, giant cell carcinoma).

Immunohistochemistry

Immunohistochemical staining was conducted by Ventana autostainer model Discover XT ™ (Ventana Medical System, Tuscan, Arizona) with enzyme labeled biotin streptavidin system and solvent resistant DAB Map kit by using mouse monoclonal Hsp27 antibody from Novocastra™ now Leica Biosystems Newcastle Ltd, Newcastle, UK and polyclonal phosphor-Hsp27 (Ser82) antibody from Cell Signaling Technology, Danvers, MA. To ensure specificity of Hsp27 and p-Hsp27 antibodies, small cell lung carcinoma and benign prostate gland basal cells tissues were used as internal negative and positive controls.

Lung Cancer Cell Lines and Reagents

A549 (EGFR wild-type and KRAS mutated: G12S) and HCC827 (EGFR mutated: delE746-A750) cells were purchased from the American Type Culture Collection and authenticated with short tandem repeat (STR) profile analysis in Jan 2013 by Genetic Resources Core Facility at John Hopkins. Cells were maintained in RPMI-1640 media (Invitrogen Life Technologies) containing 5% fetal bovine serum (FBS; Invitrogen Life Technologies). Erlotinib was purchased from LC Laboratories. A549 cell lines overexpressing Hsp27 ($A549_{Hsp27}$) were developed by stably transfecting cells with an Hsp27 vector by lentivirus transfection, as previously described [52]. $HCC827_{Resistant}$ cell lines were developed by maintaining $HCC827_{Parental}$ in 500nM erlotinib for 3 months. Genomic sequencing was done to confirm cell line identity. Antibodies: anti-HSF-1 from Santa Cruz Biotechnology; anti-Hsp27 from StressGen; anti- phospho-EGFR (Tyr1068), anti-EGFR, anti-cleaved PARP, anti-phospho-Hsp27 (Ser82), anti-cleaved caspase3, anti-caspase3, anti-phospho-ERK and anti-phospho-Akt (Ser423) were purchased from Cell Signaling Technology; and anti-β-Actin from Sigma-Aldrich.

ASO Transfection

Cells were transfected with antisense as described previously [53]. Hsp27 ASO and scrambled (ScrB) control oligonucleotide sequences were manufactured by ISIS Pharmaceuticals (Carlsbad, CA, USA) and supplied by OncoGenex Technologies (Vancouver, British Columbia, Canada). The sequence of OGX-427 corresponds to the human Hsp27 translation initiation site (5′-GGGACGCGGCGCTCGGTCAT-3′). The sequence of heat shock factor 1 (HSF-1) siRNA corresponds to the human HSF-1 site (sc-35611; Santa Cruz Biotechnology). A scrambled siRNA (5‘-CAGCGCUGACAACAGUUUCAU-3‘; Dharmacon) was used as a control for RNA interference experiments. Transfections were performed by using Oligofectamine (Invitrogen), as previously described [54].

Western Blot Analysis

Total proteins were extracted using RIPA buffer (50mM Tris, pH 7.2, 1% NP-40, 0.1% deoxycholate, 0.1% SDS, 100mM NaCl, Roche complete protease inhibitor cocktail) and

centrifuged to remove the insoluble material. Western Blots analysis was performed as described previously [53].

Quantitative reverse transcriptase PCR

RNA extraction and reverse transcriptase PCR (RT-PCR) were carried out as described previously [42]. Real-time monitoring of PCR amplification of cDNA was carried out using the following primer pairs and probes: *Hsp27* (Hs03044127_g1), *HSF1* (Hs00232134_m1), and *GAPDH* (Hs03929097_g1; Applied Biosystems) on the ABI PRISM 7900 HT Sequence Detection System (Applied Biosystems) with a TaqMan Gene Expression Master Mix (Applied Biosystems). Target gene expression was normalized to glyceraldehyde-3-phosphate dehydrogenase (*GAPDH*) levels in the respective samples as an internal control. The results are representative of at least 3 independent experiments.

***In Vitro* Cell Growth Assay**

Cells were plated in 12-well plates, and transfected with siRNA for 1 day or ASO for 2 days as indicated followed by erlotinib treatment at various concentrations for 48 hours. For VPC-27 experiments, cells were plated in 96-well plates and treated with VPC-27, erlotinib or the combination of the two drugs. Cell viability was then assessed using crystal violet assay as described previously [55]. Absorbance was determined with a micro-culture plate reader (Becton Dickinson Labware) at 560 nm. Changes in cell viability were calculated as percentage relative to the vehicle-treated cells. Each assay was performed in triplicate. The combination index (CI) was evaluated using CalcuSyn dose–effect analysis software (Biosoft) as described previously [55]. CI was calculated at ED50, ED75 and ED90.

Cell Cycle Analysis

Cell cycle populations were analyzed by propidium iodide–staining using flow cytometry as previously described [53].

Animal manipulation and Assessment of *In Vivo* Tumor Growth

For *in vivo* xenograft studies, 6x 10^6 A549 cells were inoculated s.c. in the flank of 6- to 8-week-old male athymic nude mice (Harlan Sprague Dawley, Inc.) via a 27-gauge needle under

isoflurane anesthesia. When tumors reached 100mm^3, mice were randomly selected for treatment with 50 mg/kg erlotinib (formulated in 0.5% methylcellulose + 0.1% Tween-80) orally administered once daily for 5 days per week and 15 mg/kg OGX-427 or ScrB injected i.p. once daily for 7 days and three times per week thereafter. Each experimental group consisted of 8 mice. For VPC-27 in vivo experiment, HCC827 cells were inoculated s.c. in the flank of 6-8 weeks old female athymic mice, as described above. When tumors reached 150-200 mm^3, mice were randomized to receive erlotinib 15 mg/Kg, VPC-27 10 mg/kg or the combination of the drugs (formulated in 0.5% methylcellulose + 0.1% Tween-80) orally administered, 3 days a week. Each experimental group consisted of 8 mice. Tumor volume measurements were performed once weekly for A549 and twice weekly for HCC827 and calculated by the formula length x width x depth x 0.5236. Data points were expressed as average tumor volume ± SEM. All animal procedures were performed according to the guidelines of the Canadian Council on Animal Care and with appropriate institutional certification.

Luciferase assay

HCC827 and A549 cells were transfected with HSE luciferase plasmid and pRL-TK as internal control using lipofectin reagent (Invitrogen) followed by erlotinib treatment for 24 hrs at the indicated concentrations. The luciferase activity was measured using a dual-luciferase reporter assay system (Promega) and a microplate luminometer (Tecan). The results are representative of 3 independent experiments.

Statistical Analysis

Differences between the two groups were compared using Student's t-test and Mann-Whitney U test. For the in vivo analysis ANOVA test was used. All statistical calculations were performed using Statview 5.0 software (Abacus Concepts, Inc.), and P values < 0.05 were considered significant.

RESULTS

Identification of new small molecule inhibitors of Hsp27

In order to identify functional Hsp27 inhibitors, focused small molecule libraries were first screened using a combined Fluorescence Resonance Electricity Transmission (FRET) and Fluorescence Polarization (FP) based assays. The compounds that passed the combined screening were further analyzed using protein aggregation and Hsp27 trypsin digestion. Only one of 1,280 small molecules tested, VPC-27, passed all the phases of the screening. FRET assay relies on the distance-dependent transfer of energy from a donor to an acceptor molecule (in our experiment Rhodamine Red and QSY21, respectively). Due to its sensitivity to distance, FRET has been used to investigate molecular interactions [56]. Two pools of purified Hsp27 were labelled with QSY21 (Hsp27-QSY21) and Rhodamine Red (Hsp27-RR). FRET assay results for VPC-27 showed that this molecule affects Hsp27 fluorescence quenching of Rhodamine Red by QSY-21 when the two protein pools are mixed. This confirms that VPC-27 is able to interact to Hsp27 (Fig. 1).

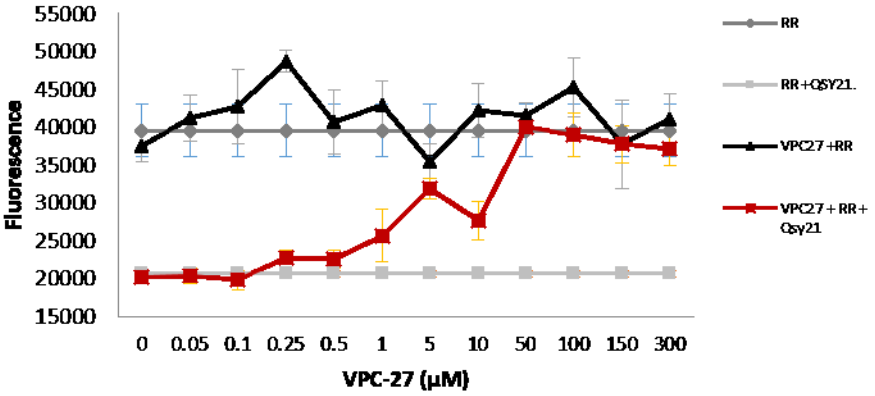

Figure 1. VPC-27 interacts with Hsp27. A mixture of Hsp27-RR and Hsp27-QSY21 were used as negative control (gray squares), Hsp27-RR alone (grey diamonds) or combined with VPC-27 (black triangles) as positive control. When a drug interferes with Hsp27 ability to exchange subunit, we observed a reduced quenching of the Rhodamine Red signal with increased VPC-27 concentrations (red squares).

Hsp27 binds to unfolded proteins, inhibiting proteins aggregation, precipitations and degradation [29]. Using FP assay we evaluated the ability of VPC-27 to inhibit the interaction of Hsp27 with unfolded insulin. As showed in figure 2A, the addiction of VPC-27 to wt-Hsp27 and insulin-

FITC, significantly decreased the formation of the Hsp27-insulin complex, as revealed by reduction of polarization. Moreover, to confirm the same effect on other proteins, we used MEF HSF1-/- cells. These cells do not express HSF-1, the main transcription factor for Hsp27, and were used as source of cellular proteins. As showed in figure 2B, after the addition of Hsp27 to the protein lysate, aggregation was significantly inhibited. Interestingly, VPC-27 treatment reverted Hsp27 effects, increasing the protein aggregation. These data demonstrated that VPC-27 affects Hsp27 ability to interact to unfolded proteins, one of the most important biological functions of Hsp27.

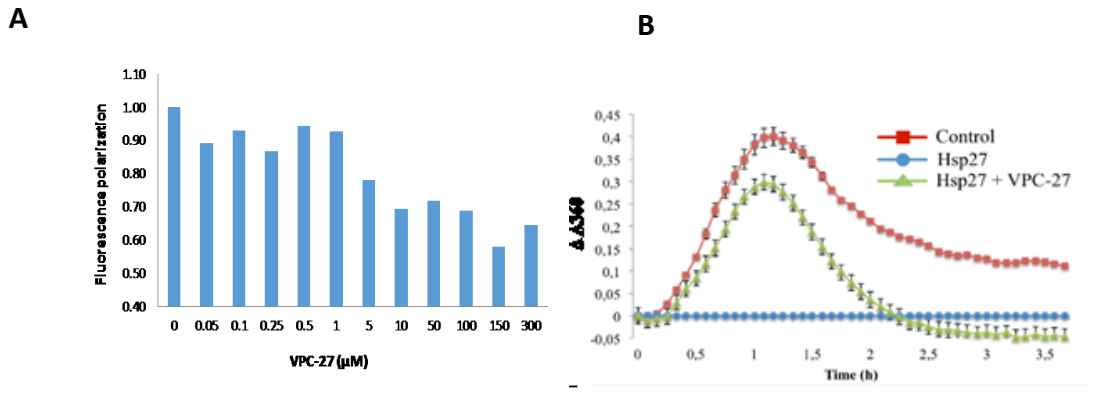

Figure 2. VPC-27 interferes with Hsp-27 - unfolded proteins binding. (A) wt-Hsp27 was incubated with Insulin-FITC and 10µM of TCEP to induce Insulin unfolded aggregation. Fluorescence polarization of Insulin was evaluated after treatment with increasing concentrations of VPC-27. (B) Protein lysate enriched with BSA from MEF HSF1-/- cells not expressing Hsp27 was used as source of proteins. The assay was conducted adding Hsp27 and DTT at 10 uM to induce protein aggregation in presence of VPC-27 10 µM or DMSO. MEF HSF1-/- cells lysate, BSA and DTT without Hsp27 were used as negative control. Results were adjusted by Hsp27 values alone.

VPC-27 interferes with Hsp27 depolymerisation and reduces Hsp27 phosphorylation

Hsp27 activity is triggered by Hsp27 phosphorylation that is able to shift the equilibrium of the large polymers to small oligomers and expose the hydrophobic surface of the protein in order to enhance its chaperone activity [31, 34]. To test whether VPC-27 affected or not Hsp27 phosphorylation, HCC827 NSCLC cancer cells were treated with increasing concentration of the drug for 24 hours in basal condition (Fig. 3A) and after Hsp27 phosphorylation stimulation using TNF-α or Heat shock (Fig. 3 B). VPC-27 was able to reduce Hsp27 phosphorylation in basal condition and to prevent it in presence of stress stimuli, confirming its activity on Hsp27 activation.

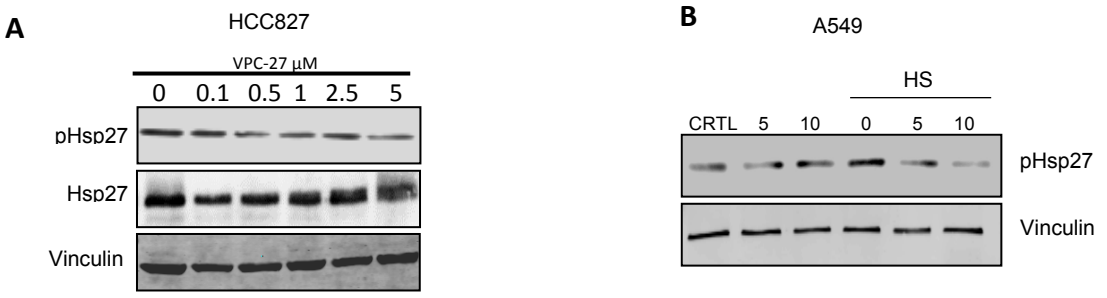

Figure 3. VPC-27 inhibits Hsp27 phosphorylation. Western Blotting analysis shows the dose-dependent effect of VPC-27 on Hsp-27 phosphorylation in NSCLC cell lines HCC827 in basal condition (A) and in A549 after Heat Shock (B). Cells were treated in RPMI with 2% of FBS with VPC-27 or DMSO for 24 hours. Proteins were extracted using RIPA buffer. Vinculin was used as loading control

Moreover, to confirm the effect of VPC-27 on Hsp27 polymerization, we analyzed the distribution of the different oligomers of Hsp27 in a glycerol gradient gel with and without VPC-27 treatment. Interestingly, we observed a shift of WT Hsp27 from the smaller to the bigger oligomers in HCC827 cells after VPC-27 treatment.

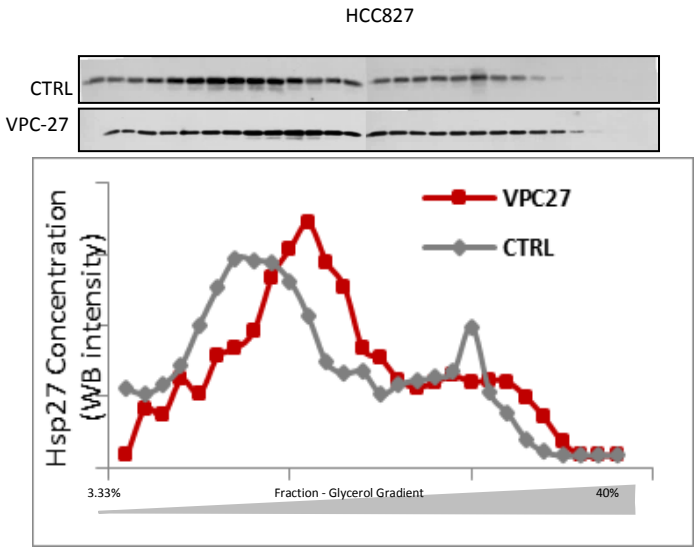

Figure 4. VPC-27 affects Hsp27 de-polymerisation. Whole protein lysate from HCC827 cells treated with DMSO or VPC-27 was added to a solution containing increasing glycerol concentrations (from 40 to 3.33 %). The fractions were centrifuged for 18hours at 36,000 RPM (160 000 x G) using SW41Ti swing bucket rotor. The fractions collected from the different glycerol gradient were loaded in a polyacrylamide gel for western blotting analysis. The graphical representation of the glycerol gradient WB shows VPC-27 treatment inhibits Hsp27 to depolymerisation from large to smaller forms.

Hsp27 and phospho-Hsp27 are highly expressed in human NSCLC.

Hsp27 has been reported to be highly and uniformly expressed in several cancers [57-61]. To assess the distribution of Hsp27 and phospho-Hsp27 expression in human NSCLC, we performed immunostaining of human NSCLC spotted on tissue microarrays (TMA). Positive Hsp27 staining was noted in 176 of 214 squamous cell carcinomas (82.2%), 139 of 195 adenocarcinomas (71.3%) and 21 of 31 large cell carcinomas (67.7%) (Fig. 5A). Positive phospho-Hsp27 staining was observed in 184 of 212 squamous cell carcinomas (86.8%), 147 of 184 adenocarcinomas (79.9%) and 27 of 31 large cell carcinomas (87.1%) (Fig. 5B). These data suggest that both Hsp27 and phospho-Hsp27 are frequently expressed in NSCLC.

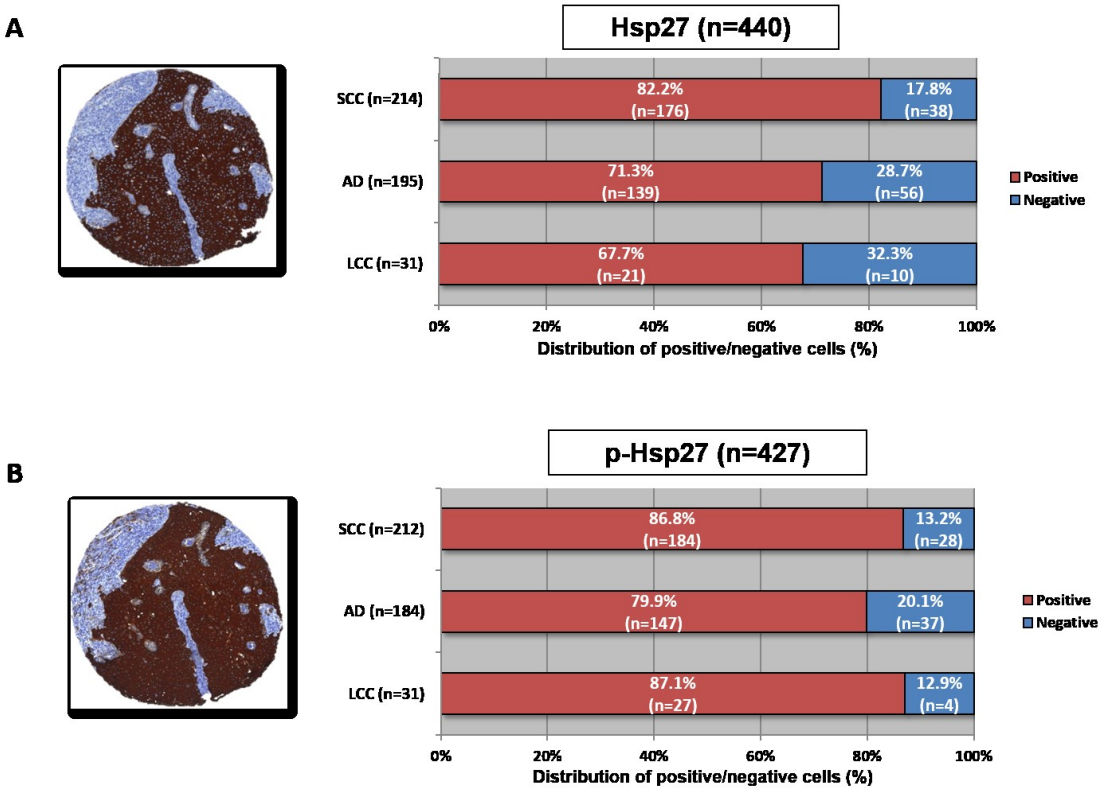

Figure 5. Hsp27 and phosphorylated Hsp27 expression in NSCLC. (A) Paraffin-embedded tissue blocks were used to construct a duplicate core tissue microarray (TMA). Hsp27 expression was evaluated in 440 NSCLC tissues. H&E-stained sections were reviewed and sub-classified as follows: 214 squamous cell carcinoma (SCC), 195 adenocarcinoma (AD) and 31 large cell carcinoma (LCC). (B) phospho-Hsp27 expression was evaluated in 427 NSCLC tissues. H&E-stained sections were reviewed and sub-classified as follows: 212 SCC, 184 AD and 31 LCC.

Erlotinib induces Hsp27 expression in A549 and HCC827 cells via HSF-1 activation.

To evaluate the effect of erlotinib on Hsp27 expression and phosphorylation, we used erlotinib-resistant A549 (IC_{25} = 4.2μM) and erlotinib-sensitive HCC827 NSCLC cell lines (IC_{25} = 8nM). Erlotinib caused a clear decrease of EGFR phosphorylation associated with a time- and dose-dependent increase of total Hsp27 and phospho-Hsp27 with a parallel increase of apoptosis as detected by cleaved PARP. (Fig. 6A)

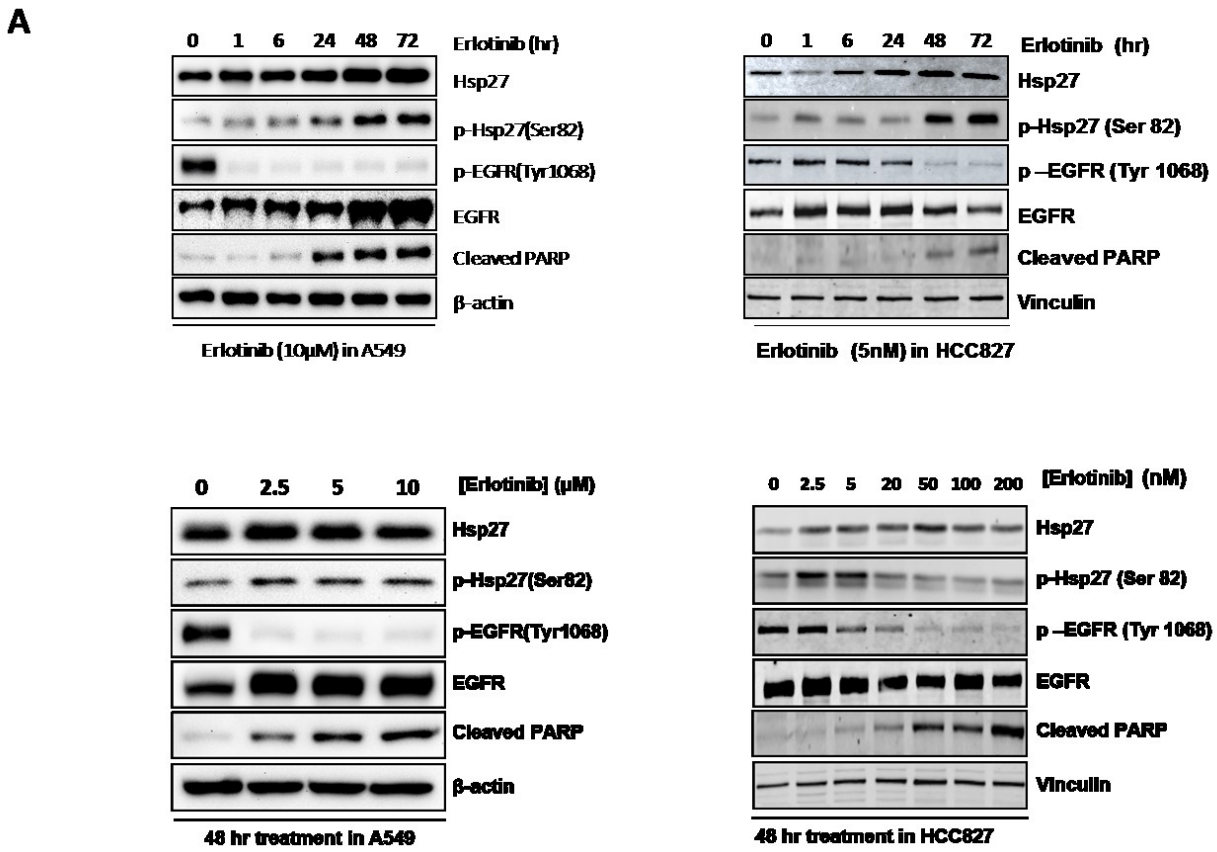

Figure 6. Erlotinib induces Hsp27/phospho-Hsp27 expression. (A) A549 (left panels) and HCC827 (right panels) cells were treated with erlotinib for up to 72h (upper panels) or for 48 H at increasing doses (lower panels), and Western Blots were performed with antibodies against p-Hsp27, total Hsp27, P-EGFR, total EGFR, Cleaved PARP. β-actin and vinculin were used as loading control.

Because HSF-1 is a key regulator of Hsp27 expression, we evaluated the effect of erlotinib on HSF-1 activity. Erlotinib led to increased HSF-1 and Hsp27 both at the protein (Fig. 7A, left panel) and mRNA levels in A549 and HCC827 cell lines (Fig. 7A, right panel). Moreover,

silencing HSF-1 using siRNA abrogated erlotinib-induced up-regulation of Hsp27 (Fig. 7B). Hsp27 can be phosphorylated by p90Rsk downstream of pAkt and pErk [39], two pathways downstream of pEGFR, and therefore inhibited by erlotinib. While levels of pAkt and pErk do not increase after erlotinib, increase of pHsp27 reflect increased HSF-1 mediated transcription of total Hsp27. Collectively these data indicate that stress-induced activation of HSF-1 by erlotinib leads to increased total Hsp27 levels and a consequent increase in p-Hsp27. This finding, in addition to the positive staining in TMA samples from a variety of NSCLC, implicates Hsp27 in erlotinib resistance and highlights it is a therapeutic target in combination therapy with EGFR TKI.

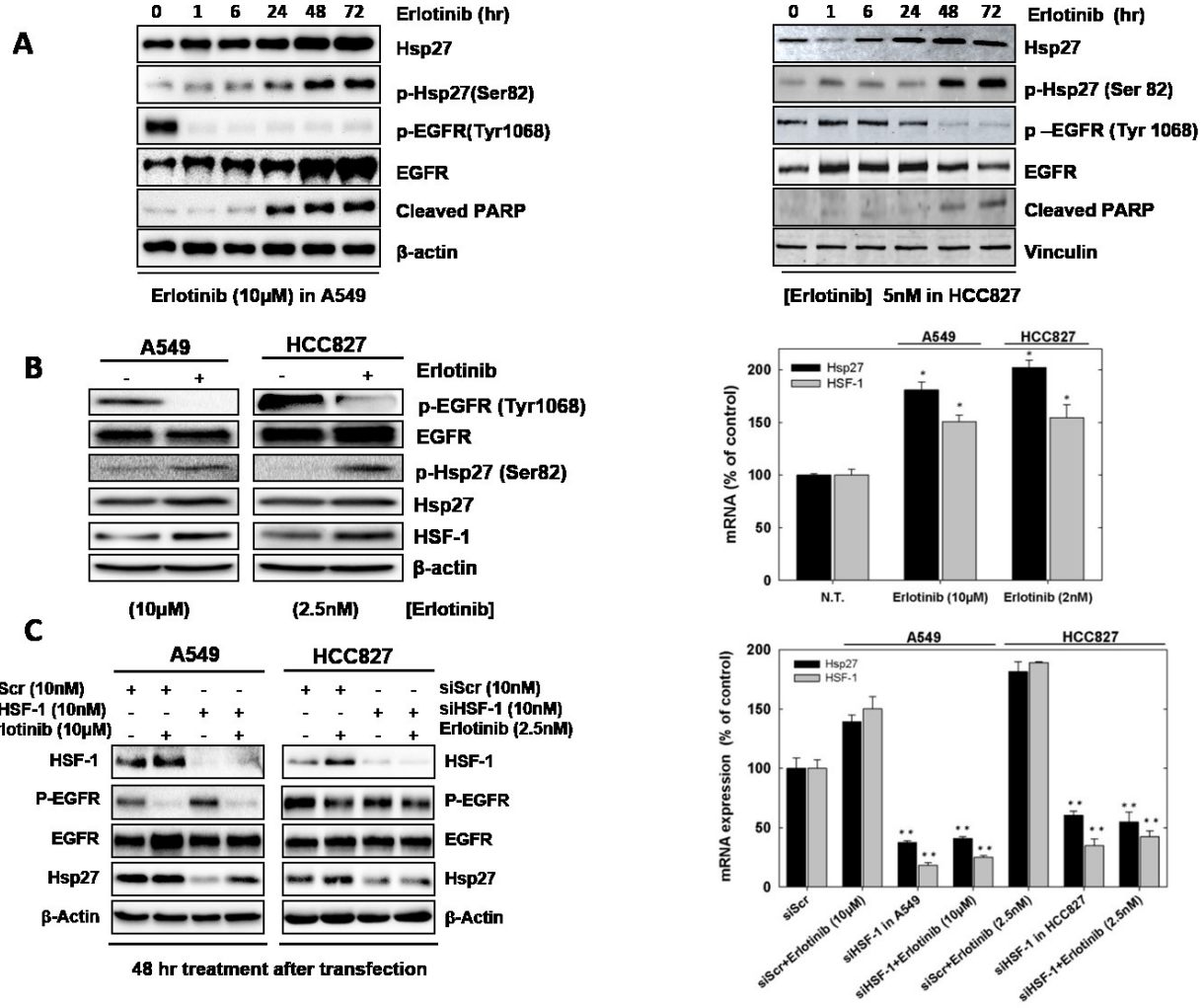

Figure 7. Erlotinib induces Hsp27 expression via activation of HSF-1. (A) A549 and HCC827 cells were treated with erlotinib for 48 hours. (Left panel) Western Blots were performed against p-EGFR, total EGFR, p-Hsp27, total Hsp27, HSF-1, and β-actin was used as loading control. (Right panel) Hsp27 and HSF-1 mRNA levels were measured by real time PCR 48h after treatment. (B) A549 and HCC827 cells were transfected daily with 20nM HSF-1 siRNA or Scramble siRNA for 1 day, followed by erlotinib treatment for 48 hours. (Left panel) HSF-1, pEGFR, total EGFR, Hsp27 and β-actin as loading control were detected by Western Blot analysis. (Right panel) mRNA levels were analyzed by real time PCR 48h after treatments. Bars, SD. ** and *, differ from control $P < 0.01$ and $P < 0.05$, respectively.

Hsp27 overexpression reduces erlotinib-induced cell death.

We previously reported that Hsp27 overexpression promotes cell survival and confers resistance to paclitaxel in prostate and bladder cancer cell lines [38, 43]. Here we investigated the effects of Hsp27 over-expression on A549 cell growth in the presence of erlotinib by comparing cell viability of a stably transfected A549 cell line ($A549_{Hsp27}$) to $A549_{Empty}$ controls after increasing doses of erlotinib. Cell viability curves in figure 8A confirm that $A549_{Hsp27}$ cells are more resistant to erlotinib compared to control $A549_{Empty}$ cells. Moreover, western blot analysis (Fig. 8B) indicates reduced PARP cleavage at 10 and 20 μM erlotinib in the $A549_{Hsp27}$ *vs*. $A549_{Empty}$ cell lines confirming that overexpression of Hsp27 protects lung cancer cells from erlotinib-induced apoptosis.

To better evaluate the role of Hsp27 in erlotinib resistance we established an HCC827 resistant cell line (IC_{25} = 1μM) by maintaining HCC827 parental cells in 500nM erlotinib for 3 months (Fig. 8C). Fig 8D shows reduced cleaved PARP and increased expression of Hsp27 in $HCC827_{resistant}$ cells compared to parental. These findings further implicate Hsp27 in erlotinib resistance both when Hsp27 becomes endogenously over-expressed in response to treatment ($HCC827_{resistant}$) and when it is highly expressed via stable transfection ($A549_{Hsp27}$).

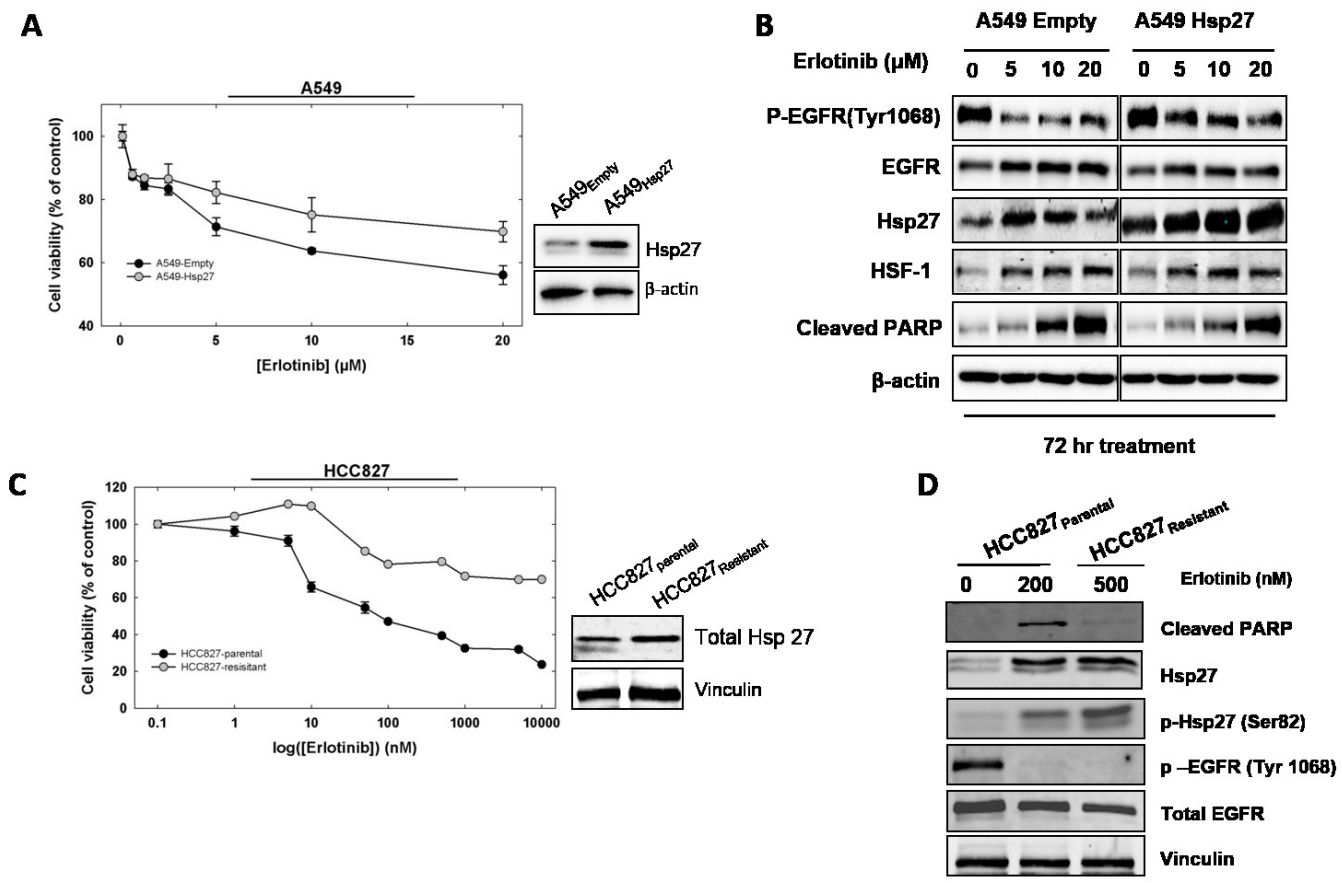

Figure 8. Hsp27 overexpression induces erlotinib resistance. (A) A549 cells were stably transfected either with an empty vector ($A549_{Empty}$) or with a vector containing wild-type Hsp27 ($A549_{Hsp27}$). Cell viability was determined after increasing erlotinib doses 72h after treatment. (B) p-EGFR, total EGFR, Hsp27, cleaved PARP, and β-actin as loading control were detected by Western Blot in both cell lines after 72h erlotinib treatment. (C) HCC827 erlotinib-resistant cell lines ($HCC827_{resistant}$) were established maintaining $HCC827_{parental}$ cells in 500nM erlotinib for 3 months. Hsp27 levels were measured by Western Blots (insert). Cell viability was determined after increasing erlotinib doses 72h after treatment. (D) Cleaved PARP, Hsp27, p-Hsp27, p-EGFR, total EGFR, and vinculin as loading control were detected by Western Blot for resistant cells at 500nM erlotinib and parental cells at 0 and 72h after 200nM erlotinib.

Hsp27 inhibition, by OGX-427 or VPC-27, sensitizes both HCC827 and A549 to erlotinib.

Since the preceding results links Hsp27 to erlotinib resistance we hypothesized that co-targeting this chaperone in combination with EGFR TKI will increase erlotinib efficacy. Cell viability was assessed in A549 and HCC827 cells after erlotinib or OGX-427 mono- and combination-therapy. OGX-427 leads to increased cell death compared to single agent therapy when used in combination with erlotinib (Fig. 9A). Combination Index, calculated at a ratio OGX-427:erlotinib 1:200 for A549 and 20:1 for HCC827, confirms a synergistic effect for this drug

combination (Fig. 9B). Increased levels of cleaved PARP and caspase 3 assessed by Western Blotting (Fig. 9C), together with increased subG$_0$ apoptotic fraction assessed by PI staining–based FACS analysis (Fig. 9D) confirmed that OGX-427 enhances erlotinib-induced apoptosis.

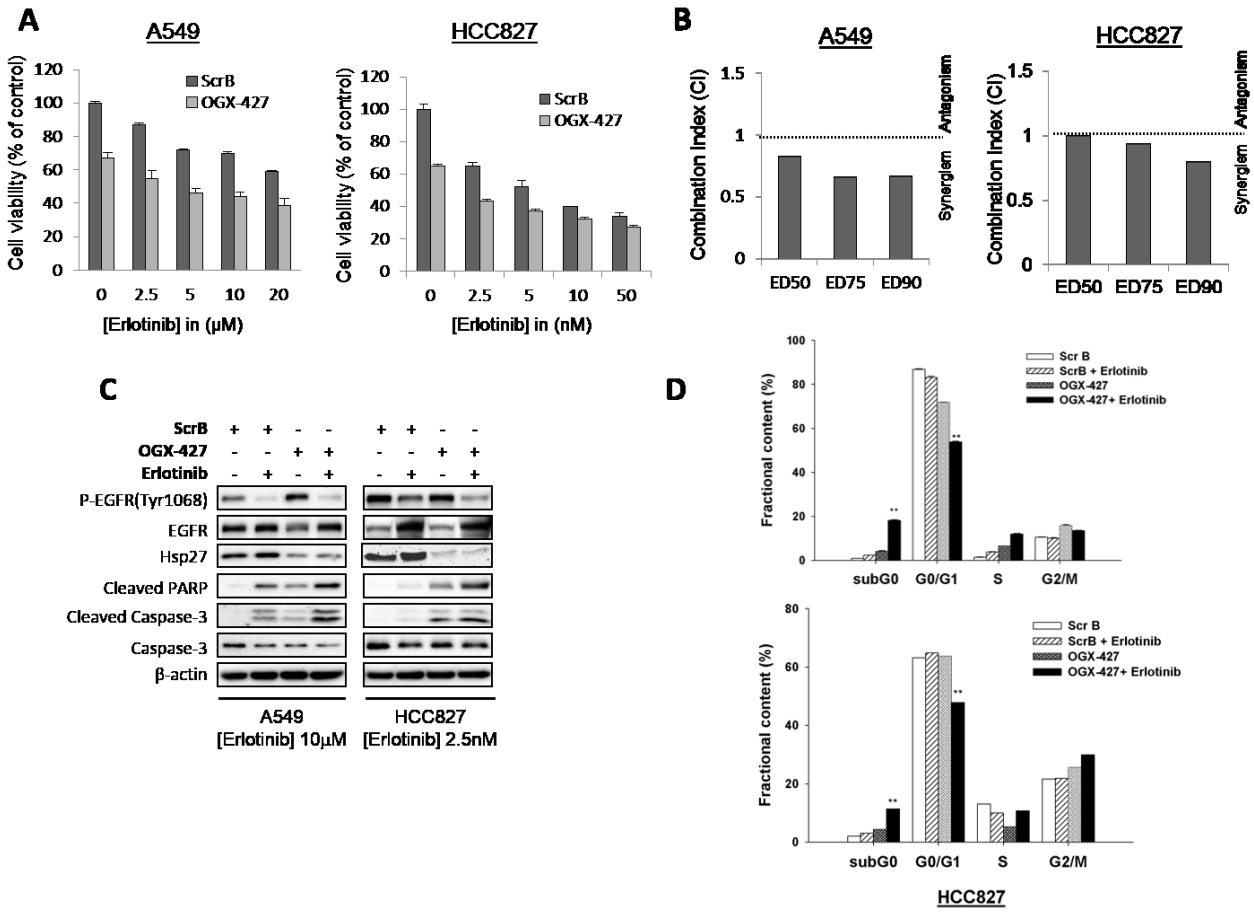

Figure 9. OGX-427 sensitizes both HCC827 and A549 to erlotinib. (A) A549 and HCC827 cells were transfected with 50nM OGX-427 or ScrB for 2 days and treated with the indicated concentration of erlotinib for 48 hours after the second transfection. Cell viability was determined by crystal violet assay 48h after erlotinib treatment. (B) Combination index analysis for erlotinib and OGX-427 treatment in A549 and HCC827 cell lines was performed according to the Chou and Talalay method [49]. (C) p-EGFR, total EGFR, total Hsp27, cleaved PARP, cleaved caspase-3, caspase-3 and β-actin, as loading control, were detected by Western Blot analysis. Inhibition of erlotinib-induced Hsp27 enhances cell apoptosis in both A549 and HCC827. (D) Cells were transfected with 50nM OGX-427 or ScrB for 2 days and treated with erlotinib (A549 at 10μM and HCC827 at 2.5nM) for 48 hours after the second transfection. Flow cytometry analysis of A549 and HCC827 show an increase in subG0 and decrease in G0/G1. SD. ** and *, differ from control ($P < 0.01$ and $P < 0.05$, respectively).

The same experiments on cell viability was conducted in HCC827 and A549 cells combining VPC-27 and erlotinib. As demonstrated in figure 10, VPC-27 treatment had the same effect of erlotinib in both cell lines in monotherapy. However, the combination of the two drugs

significantly inhibited cell survival in both cell models, confirming that Hsp27 inhibition increases NSCLC cancer cell sensitivity to EGFR inhibitor erlotinib.

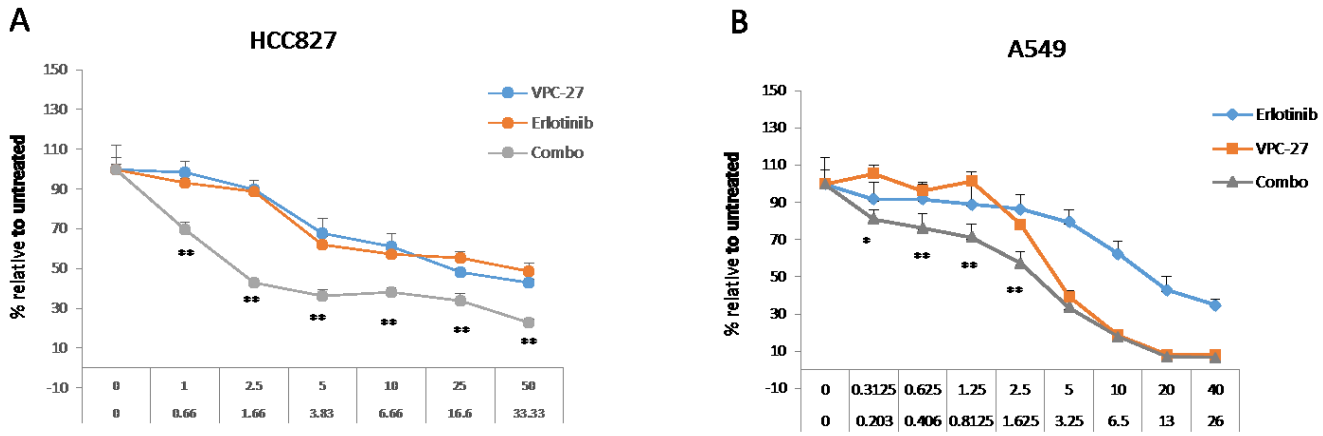

Figure 10. VPC-27 increases cells sensitivity to erlotinib. Percentage of survival cells after treatment with increasing doses of VPC-27, erlotinib or the combination of the two drugs, in HCC827 (A) and A549 (B) NSCLC cell lines. The cells were plated in 96 well plate and treated for 4 days. Cells were fixed with glutaraldehyde 1% and colored with crystal violet. The number of survived cells was evaluated measuring absorbance of crystal violet at 520 nm. Error bars: standard deviation. T- test values: * $p<0.05$, ** $p<0.001$.

Combining OGX-427 or VPC-27 with erlotinib enhances tumor growth inhibition *in vivo*

The combination effect of OGX-427 or VPC-27 and erlotinib was next evaluated in an *in vivo* model using A549 and HCC827 xenografts, respectively. Tumor-bearing mice were randomly assigned to groups treated with ScrB+Diluent, ScrB+Erlotinib, OGX-427+Diluent or OGX-427+Erlotinib when A549 tumors reached 100 mm^3. Mean tumor volume were similar in all groups at baseline and all treatments were performed for 7 weeks. Consistent with *in vitro* findings, OGX-427 was able to reduce Hsp27 protein level and the combination therapy of OGX-427 plus erlotinib significantly reduced tumor growth rates (Fig. 11A-C) compared with all other groups (P=0.0002, 0.03 and 0.01 against ScrB+Diluent, ScrB+Erlotinib and OGX-427+Diluent, respectively). Moreover, OGX-427 plus erlotinib-treated tumors had higher apoptotic rates as shown by increased TUNEL staining compared with the other groups (Fig. 9D). These studies indicated that this combination treatment significantly delays growth and increases apoptotic rates of A549 xenografts.

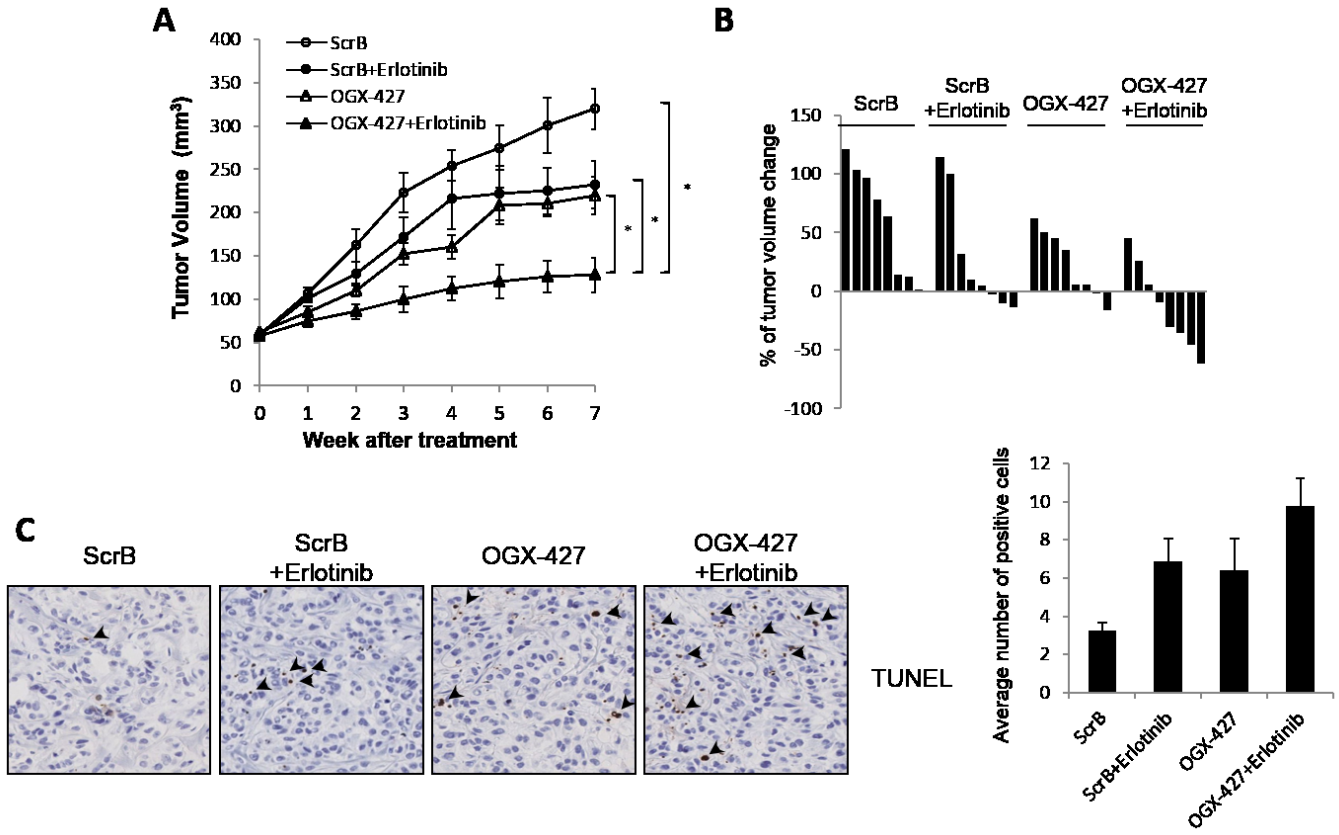

Figure 11. OGX-427 plus erlotinib delays A549 xenograft growth in vivo. (A) A549 cells were inoculated s.c. and when tumor volume reached 50-100mm3, mice were treated with scrambled (ScrB) control+diluent, ScrB+erlotinib, OGX-427+diluent or OGX-427+erlotinib as described in Materials and Methods. Each data point represents the mean tumor volume in each group containing 8 mice ± SEM. *, differ from ScrB+diluent, ScrB+erlotinib, OGX-427+diluents or OGX-427+erlotinib treatment group ($P<0.05$). (B) Tumor volume changes were evaluated three weeks after starting the treatment. We set as 0 that at which tumor volume doubled after starting the treatment. (C) Hsp27 down regulation after OGX-427 treatment was evaluated by Western Blot. Three animals were (D) Tumors were collected after 49 days and TUNEL were evaluated by immunohistochemical analysis (original magnification: x200). used as representative samples from each group.

The same effect was observed with VPC-27. HCC827 bearing mice were treated with vehicle only, erlotinib, VPC-27 or VPC-27+erlotinib when HCC827 tumors reached 150-200 mm^3. As expected, erlotinib inhibited tumor growth but interestingly also VPC-27 showed to significantly affect tumor growth as single agent. As observed in vitro, the combination of VPC-27 and erlotinib was the most active therapeutic strategy compared with all other groups (Fig. 12A). Moreover, we were able to confirm the on target effect of VPC-27 on p-Hsp27 also in vivo, as demonstrated by the reduction of the levels of p-Hsp27 evaluated by immunohistochemistry (Fig. 12B).

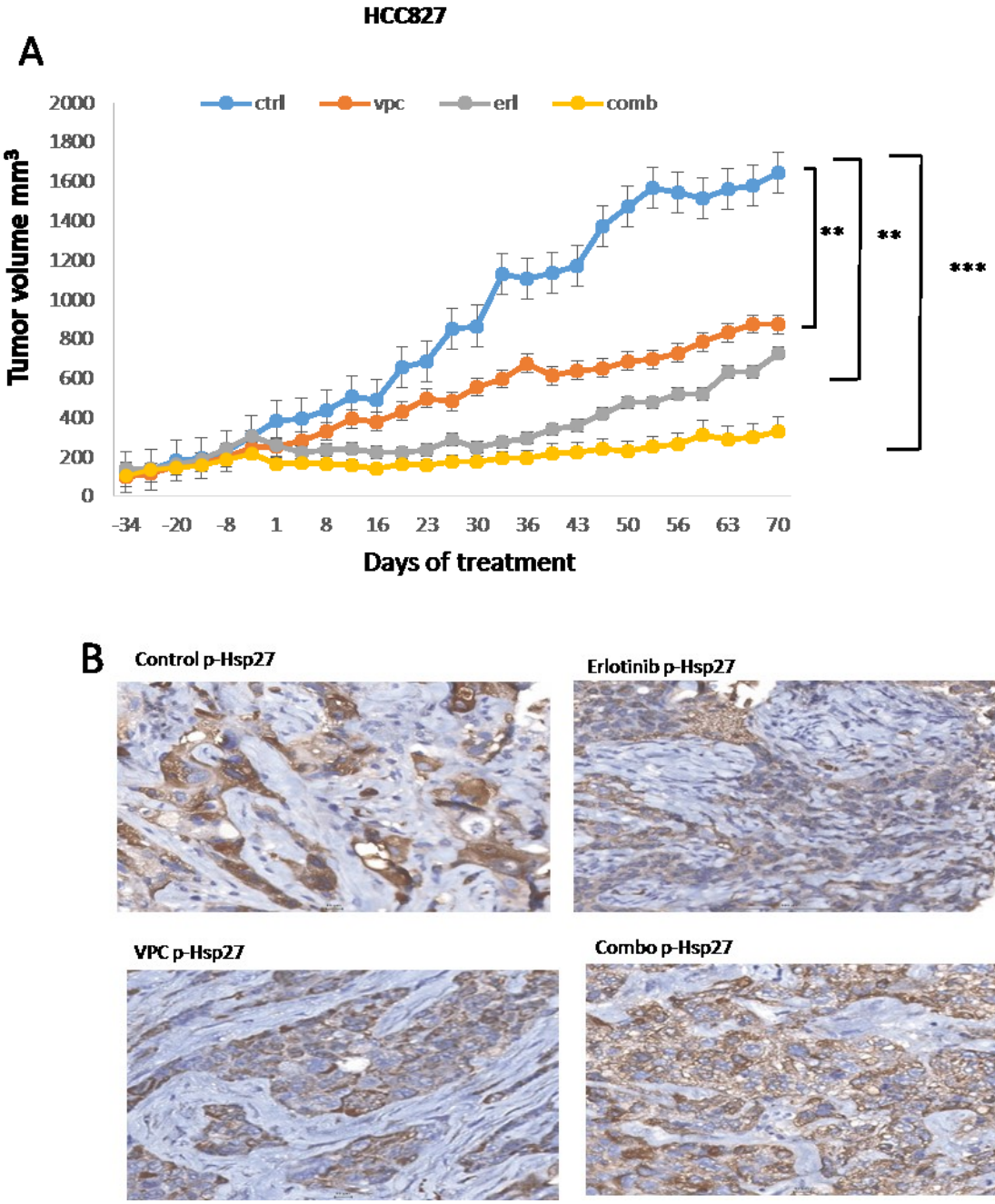

Figure 12. VPC-27 inhibits tumor growth and enhances erlotinib activity in HCC827 xenograft mice. (A) HCC827 cells were inoculated s.c. in Balbc mice and when tumor volume reached 150 mm^3 mice were treated with vehicle (ctrl), vehicle+erlotinib, vehicle+VPC-27 or VPC-27+erlotinib as described in Materials and Methods. Each data point represents the mean tumor volume in each group containing 8 mice ± SEM. **/***, differ from vehicle, erlotinib, VPC-27 or VPC-27+erlotinib treatment group (***P<0.01, P< 0.001). (B) Tumors were collected at the endpoint of the mice and p-Hsp27 was evaluated by immunohistochemical analysis. A representative sample from each group is represented.

DISCUSSION

Anti-cancer treatments induce stress responses that inhibit apoptosis and promote emergence of an acquired treatment-resistant phenotype. Molecular chaperones play key roles in these stress responses by regulating many pro-survival signaling and transcriptional networks. Two strategies have recently emerged that are revolutionizing the treatment landscape in cancer: the use of molecular-targeted agents and the selective inhibition of adaptive responses. In this work we focus on the role of treatment-induced Hsp27 expression and treatment response in NSCLC, the most common type of lung cancer and the largest cause of cancer-related death worldwide, where chemotherapy or EGFR-TKIs are first-line treatment. EGFR belongs to a family of membrane bound receptors with a tyrosine kinase domain that, when phosphorylated, activates a number of downstream pro-survival pathways including the PI3K/Akt and RAS/MAPK pathways [14, 62]. Some patients, for whom EGFR-TKI is recommended, have a mutated EGFR that is constitutively activated. For these individuals the use of EGFR-TKI is recommended over chemotherapy as first line of treatment [22-23]. Although EGFR TKIs have been shown to prolong life, most patients acquire resistance with a median progression-free survival of 10 months [63] and eventually die of metastatic disease.

Hsp27 is a stress-induced molecular chaperone that regulates many pro-survival cellular functions. Many solid tumors, including bladder, prostate, breast and colorectal cancers, express high Hsp27 levels that correlate with poor prognosis. Hsp27 maintains protein homeostasis by stabilizing protein conformation or facilitating proteasomal degradation [31-40], inhibits apoptosis by interacting with pro-apoptotic molecules like cytochrome *c* [64] or pro-caspase 3 [65], and enhances oncogenic signaling pathways such as STAT3, IGF-1, androgen receptor (AR), and eIF4E [38, 53, 66]. Consistent with these multiple cytoprotective functions, overexpression of Hsp27 renders cancer cells resistant to chemo- and hormonal- therapy [36, 38].

Since Hsp27 functions as a regulatory "hub" in multiple regulatory pathways, its inhibition will simultaneously suppress many pathways implicated in cancer progression and resistance to hormone- and chemo-therapies. Hsp27 acts through an ATP-independent mechanism and is therefore not amenable to inhibition by 17-AAG derived small molecules. Strategies to inhibit Hsp27 at the mRNA level are an alternative approach to inhibiting "non-druggable" targets; indeed, short

interfering RNA (siRNA) or antisense oligonucleotides targeting Hsp27 suppresses proliferation and EMT in prostate [33, 38, 67] and breast cancer cells [68]. Hsp27 silencing also decreases clonogenic survival and induces cell senescence in HCT116 human colon cancer [69]. Hsp27 silencing chemo-sensitizes SK-BR-3 HR breast cancer cells to Herceptin [70], A549 lung cancer cells to 17-AAG [71], MUC-3 bladder cancer cells and PC-3 prostate cancer cells to paclitaxel [43, 67]. Targeting Hsp27 is changeling because of the high dynamic structure of the protein that adapt its size to the cellular context, facilitating cancer survival. Using a combined biochemical screening, we identified the first small molecule, VPC-27, able to inhibit Hsp27. This drug affects Hsp27 phosphorylation and thus inhibits Hsp27 binding to unfolded proteins, a fundamental Hsp27 function to protect the cells from the death. However, we do not have enough data, at the moment, to understand the exact molecular mechanism of Hsp27 inhibition by this drug. The inhibition of the phosphorylation reduces the production of Hsp27 dimers, described as the most active forms [72].

Moreover, VPC-27 also modified the equilibrium of the Hsp27 oligomers, from the smallest (more active) to the biggest (less active). Whether or not this shift is the cause or the effect of the inhibition of the phosphorylation is under investigations.

In this study we show that Hsp27 and phospho-Hsp27 are commonly expressed in a TMA of 440 squamous cell carcinomas, adenocarcinomas and large cell carcinomas of the lung. We also show that treatment stress with erlotinib or chemotherapy increases Hsp27 expression via the transcription factor HSF-1 and that high levels of Hsp27 induces resistance to erlotinib. These findings implicate a role for Hsp27 in cell survival of NSCLC under EGFR inhibition, and supports testing co-targeting Hsp27 with erlotinib or other chemotherapeutics for the treatment of NSCLC. Inhibition of treatment-induced Hsp27 using OGX-427 or VPC-27 synergistically enhanced inhibitory effects of erlotinib on cell proliferation and cell viability in NSCLC cell lines *in vitro*. Similarly, combination therapy with erlotinib plus OGX-427 or VPC-27 significantly inhibited A549 and HCC827 tumor growth *in vivo* compared to monotherapy. Consistent with these results, Hsp27 is up-regulated by HSF-1 in c-MET addicted gastric cell lines when c-MET is inhibited, and functions to limit the activity of c-MET-targeted therapies [73]. In this gastric cell line, the activation of K-RAS by transfection of G12V K-RAS downstream of c-MET reverses the effect of c-MET inhibitors on Hsp27 up-regulation [73]. We observed an increase of Hsp27 even in A549 lung cancer cells that have a constitutively

activated MAP kinase pathway due to a K-RAS activating mutation (G12S), demonstrating that in A549 lung cancer cells, Hsp27 up-regulation via HSF-1 is a response to EGFR inhibition even when the MAP kinase pathway is constitutively active.

These results provide a framework for building new drug combinations based on mechanism-based interventions to overcome drug resistance, and pre-clinical proof-of-principle supporting clinical trials of OGX-427 combination regimens for lung and other cancers. OGX-427 has completed single agent and docetaxel-combination dose escalation Phase I trials in prostate, bladder, breast, and lung cancer [46-48]. OGX-427 is well tolerated, with the majority of the adverse events reported being Grade 1 or Grade 2, although a symptom complex of rigors, pruritus, and erythema during or shortly after infusion of drug has required steroid prophylaxis and/or treatment in some patients at higher doses. Preliminary data from a randomized phase II trial of OGX-427 plus prednisone in castration resistant prostate cancer reported a PSA decline ≥ 30% in 55% of patients and an acceptable safety profile [47]. Several randomized Phase II trials of OGX-427 in combination with chemotherapy are actively accruing, including untreated Stage IV NSCLC comparing carboplatin plus pemetrexed with or without OGX-427 (SPRUCE, clinicaltrials.gov NCT01829113).

CONCLUSIONS

To summarize, we have identified the first Hsp27 small molecule inhibitor, VPC-27, which showed to efficiently inhibit Hsp27 phosphorylation and leads the way for an entirely new strategy to inhibit Hsp27. Further research is ongoing to better understand the exact mechanism of action of VPC-27, a very promising drug. The functional and transcriptional inhibition of Hsp27 induces a significant inhibition of NSCLC tumor proliferation in vitro and in vivo. Overall, small molecule inhibitors of Hsp27 could represent a valid therapeutic strategy to improve survival of patients affected by metastatic NSCLC.

ACKNOWLEDGEMENTS

I gratefully acknowledge the funding sources that made this work possible:

1. Terry Fox New Frontiers Program and the Pacific Northwest Prostate Cancer SPORE NCI CA097186 to Martin Gleave.
2. Pier Luigi Tolaini Young Investigator Award from the Coalition to Cure Prostate Cancer to B. Lelj-Garolla.
3. Michael Smith Foundation 2015 Trainee Award to Lucia Nappi.

I acknowledge Dr. Martin Gleave for welcoming me in his group and for giving me the opportunity to be part of this project.

A special acknowledge to Barbara Lelj Garolla and Eliana Beraldi and all the staff of the Vancouver Prostate Centre for their support in the months that I have spent there.

I acknowledge Prof. Giovannella Palmieri and Giampaolo Tortora to have inspired me to the passion and dedication to oncology research.

I acknowledge Prof. Sabino De Placido and Roberto Bianco for the help during this doctorate.

And finally thanks to Emiddio, always by my side in these months of hard work, and to my family and friends who have always encouraged me.

REFERENCES

1. Siegel RL, Miller KD, Jemal A. CA Cancer J Clin. 2015 Jan-Feb;65(1):5-29. Epub 2015 Jan 5. Cancer statistics, 2015.

2. Howlader N, Noone AM, Krapcho M, et al. SEER Cancer Statistics Review, 1975-2012, National Cancer Institute. Bethesda, MD, based on November 2014 SEER data submission, posted to the SEER web site, April 2015.

3. Sandler A, Gray R, Perry MC, et al. Paclitaxel-carboplatin alone or with bevacizumab for non-small-cell lung cancer. N Engl J Med. 2006 Dec 14;355(24):2542-50.

4. Brahmer J, Reckamp KL, Baas P, et al. Nivolumab versus Docetaxel in Advanced Squamous-Cell Non-Small-Cell Lung Cancer. N Engl J Med. 2015 Jul 9;373(2):123-35. Epub 2015 May 31.

5. Herbst RS, Baas P, Kim DW, et al. Pembrolizumab versus docetaxel for previously treated, PD-L1-positive, advanced non-small-cell lung cancer (KEYNOTE-010): a randomised controlled trial. Lancet. 2015 Dec 18. pii: S0140-6736(15)01281-7.

6. Garon EB, Ciuleanu TE, Arrieta O, et al. Ramucirumab plus docetaxel versus placebo plus docetaxel for second-line treatment of stage IV non-small-cell lung cancer after disease progression on platinum-based therapy (REVEL): a multicentre, double-blind, randomised phase 3 trial. Lancet. 2014 Aug 23;384(9944):665-73.

7. Solomon BJ, Mok T, Kim DW, et al. First-line crizotinib versus chemotherapy in ALK-positive lung cancer. N Engl J Med. 2014 Dec 4;371(23):2167-77.

8. Scagliotti GV, Novello S, Rapetti S, et al. Current state-of-theart therapy for advanced squamous cell lung cancer. Am Soc Clin Oncol Educ Book 2013; 354–58.

9. Ciardiello F and Tortora G. EGFR antagonists in cancer treatment. N Engl J Med. 2008 Mar 13;358(11):1160-74.

10. Sequist LV, Joshi VA, Jänne PA, et al. Response to treatment and survival of patients with non-small cell lung cancer undergoing somatic EGFR mutation testing. Oncologist. 2007 Jan;12(1):90-8.

11. Lemmon MA, Schlessinger J, Ferguson KM. The EGFR family: not so prototypical receptor tyrosine kinases. Cold Spring Harb Perspect Biol. 2014 Apr 1;6(4):a020768.

12. Bae JH and Schlessinger J. Asymmetric tyrosine kinase arrangements in activation or autophosphorylation of receptor tyrosine kinases. Mol Cells. 2010 May;29(5):443-8.

13. Guo L, Kozlosky CJ, Ericsson LH, et al. Studies of ligand-induced site-specific phosphorylation of epidermal growth factor receptor. J Am Soc Mass Spectrom. 2003 Sep;14(9):1022-31.

14. Yarden Y and Sliwkowski MX. Untangling the ErbB signalling network. Nat Rev Mol Cell Biol. 2001 Feb;2(2):127-37.

15. Olayioye MA, Neve RM, Lane HA, et al. The ErbB signaling network: receptor heterodimerization in development and cancer. EMBO J. 2000 Jul 3;19(13):3159-67.

16. Sharma SV, Bell DW, Settleman J, et al. Epidermal growth factor receptor mutations in lung cancer. Nat Rev Cancer. 2007 Mar;7(3):169-81.

17. Herbst RS and Shin DM. Monoclonal antibodies to target epidermal growth factor receptor-positive tumors: a new paradigm for cancer therapy. Cancer 2002; 94: 1593– 1611.

18. Mukohara T, Engelman JA, Hanna NH, et al. Differential effects of gefitinib and cetuximab on non-small-cell lung cancers bearing epidermal growth factor receptor mutations. J Natl Cancer Inst 2005;97:1185-94.

19. Solca F, Dahl G, Zoephel A, et al. Target binding properties and cellular activity of afatinib (BIBW 2992), an irreversible ErbB family blocker. J Pharmacol Exp Ther 2012; 343: 342–50.

20. Lynch TJ, Bell DW, Sordella R, et al. Activating mutations in the epidermal growth factor receptor underlying responsiveness of non–small-cell lung cancer to gefitinib. N Engl J Med 2004; 350:2129-39.

21. Sequist LV, Yang JC, Yamamoto N, et al. Phase III study of afatinib or cisplatin plus pemetrexed in patients with metastatic lung adenocarcinoma with EGFR mutations. J Clin Oncol. 2013 Sep 20;31(27):3327-34.

22. Rosell R, Carcereny E, Gervais R, et al. Erlotinib versus standard chemotherapy as first-line treatment for European patients with advanced EGFR mutation-positive non-small-cell lung cancer (EURTAC): a multicentre, open-label, randomised phase 3 trial. Lancet Oncol. 2012 Mar;13(3):239-46.

23. Fukuoka M, Wu YL, Thongprasert S, et al. Biomarker analyses and final overall survival results from a phase III, randomized, open-label, first-line study of gefitinib versus carboplatin/paclitaxel in clinically selected patients with advanced non-small-cell lung cancer in Asia (IPASS). J Clin Oncol. 2011 Jul 20;29(21):2866-74.

24. Kobayashi S, Boggon T J, Dayaram T. EGFR mutation and resistance of non-small-cell lung cancer to gefitinib N. Engl. J. Med. 2005, 352, 786– 792.

25. Walter A O, Sjin RTT, Haringsma HJA. Discovery of a mutant-selective covalent inhibitor of EGFR that overcomes T790M-mediated resistance in NSCLC Cancer Discovery 2013, 3, 1404– 1415.

26. Shimamura T, Lowell AM, Engelman JA et al. Epidermal growth factor receptors harboring kinase domain mutations associate with the heat shock protein 90 chaperone and are destabilized following exposure to geldanamycins. Cancer Res 2005;65:6401-8.

27. Hickey E, Brandon SE, Potter R, et al. Sequence and organization of genes encoding the human 27 kDa heat shock protein. Nucleic Acids Res 1986;14:4127-45.

28. Trinklein ND, Chen WC, Kingston RE et al. Transcriptional regulation and binding of heat shock factor 1 and heat shock factor 2 to 32 human heat shock genes during thermal stress and differentiation. Cell Stress Chaperones 2004;9:21-8.

29. Kostenko S. and U. Moens, Heat shock protein 27 phosphorylation: kinases, phosphatases, functions and pathology. Cell Mol Life Sci, 2009. 66(20): p. 3289-307.

30. Doshi BM, Hightower LE, Lee J. The role of Hsp27 and actin in the regulation of movement in human cancer cells responding to heat shock. Cell Stress Chaperones. 2009 Sep;14(5):445-57.

31. Lelj-Garolla B. and A.G. Mauk. Roles of the N- and C-terminal sequences in Hsp27 self-association and chaperone activity. Protein Sci, 2012. 21(1): p. 122-33.

32. Hayashi N, Peacock JW, Beraldi E, et al. Hsp27 silencing coordinately inhibits proliferation and promotes Fas-induced apoptosis by regulating the PEA-15 molecular switch. Cell Death Differ, 2012. 19(6): p. 990-1002.

33. Shiota M, Bishop JL, Nip KM et al. Hsp27 Regulates Epithelial Mesenchymal Transition, Metastasis, and Circulating Tumor Cells in Prostate Cancer. Cancer Research, 2013. 73(10): p. 3109-3119.

34. Theriault JR, Lambert H, Chávez-Zobel AT, et al. Essential role of the NH2-terminal WD/EPF motif in the phosphorylation-activated protective function of mammalian Hsp27. J Biol Chem, 2004. 279(22): p. 23463-71.

35. Zoubeidi, A. and M. Gleave, Small heat shock proteins in cancer therapy and prognosis. Int J Biochem Cell Biol, 2012. 44(10): p. 1646-56.

36. Andrieu C,Taieb D, Baylot V, et al. Heat shock protein 27 confers resistance to androgen ablation and chemotherapy in prostate cancer cells through eIF4E. Oncogene, 2010. 29(13): p. 1883-96.

37. Rocchi P, So A, Kojima S, et al. Heat shock protein 27 increases after androgen ablation and plays a cytoprotective role in hormone-refractory prostate cancer. Cancer Res, 2004. 64(18): p. 6595-602.

38. Rocchi P, Beraldi E, Ettinger S, et al. Increased Hsp27 after androgen ablation facilitates androgen-independent progression in prostate cancer via signal transducers and activators of transcription 3-mediated suppression of apoptosis. Cancer Res, 2005. 65(23): p. 11083-93.

39. Zoubeidi A, Zardan A, Wiedmann RM, et al. Hsp27 promotes insulin-like growth factor-I survival signaling in prostate cancer via p90Rsk-dependent phosphorylation and inactivation of BAD. Cancer Res, 2010. 70(6): p. 2307-17.

40. Kumano M, Furukawa J, Shiota M, et al. Cotargeting stress-activated Hsp27 and autophagy as a combinatorial strategy to amplify endoplasmic reticular stress in prostate cancer. Mol Cancer Ther, 2012. 11(8): p. 1661-71.

41. Gleave M.E. and B.P. Monia, Antisense therapy for cancer. Nat Rev Cancer, 2005. 5(6): p. 468-79.

42. Lamoureux F, Thomas C, Yin MJ, et al. Suppression of heat shock protein 27 using OGX-427 induces endoplasmic reticulum stress and potentiates heat shock protein 90 inhibitors to delay castrate-resistant prostate cancer. Eur Urol. 2014 Jul;66(1):145-55.

43. Kamada M, So A, Muramaki M, et al. Hsp27 knockdown using nucleotide-based therapies inhibit tumor growth and enhance chemotherapy in human bladder cancer cells. Mol Cancer Ther, 2007. 6(1): p. 299-308.

44. Hadaschik B.A, Jackson J, Fazli L, et al. Intravesically administered antisense oligonucleotides targeting heat-shock protein-27 inhibit the growth of non-muscle-invasive bladder cancer. BJU Int, 2008. 102(5): p. 610-6.

45. Choi DH, Ha JS, Lee WH, et al. Heat shock protein 27 is associated with irinotecan resistance in human colorectal cancer cells. FEBS Lett, 2007. 581(8): p. 1649-56.

46. Chi KN, Yu EY, Jacobs C, et al. A phase I dose-escalation study of apatorsen (OGX-427), an antisense inhibitor targeting heat shock protein 27 (Hsp27), in patients with castration-resistant prostate cancer and other advanced cancers. Ann Oncol. 2016 Feb 18.

47. Chi KN, Hotte SJ, Ellardet S, et al. A randomized phase II study of OGX-427 plus prednisone (P) versus P alone in patients (pts) with metastatic castration resistant prostate cancer (CRPC). Journal of Clinical Oncology, 2012. 30(15).

48. So A, Black P, Chi K, et al. A phase I trial of intravesical antisense oligonucleotide targeting heat shock protein 27 (OGX-427) for the treatment of non-muscle-invasive bladder cancer. J Clin Oncol 30, 2012 (suppl 5; abstr 286).

49. McDonald ET, Bortolus M, Koteiche HA, et al. Sequence, structure, and dynamic determinants of Hsp27 (HspB1) equilibrium dissociation are encoded by the N-terminal domain. Biochemistry, 2012. 51(6): p. 1257-68.

50. Giese KC, Basha E, Catague BY, et al. Evidence for an essential function of the N terminus of a small heat shock protein in vivo, independent of in vitro chaperone activity. Proc Natl Acad Sci U S A, 2005. 102(52): p. 18896-901.

51. Lelj-Garolla B. and A.G. Mauk. Self-association and chaperone activity of Hsp27 are thermally activated. J Biol Chem, 2006. 281(12): p. 8169-74.

52. Trinklein ND, Chen WC, Kingston RE et al. Transcriptional regulation and binding of heat shock factor 1 and heat shock factor 2 to 32 human heat shock genes during thermal stress and differentiation. Cell Stress Chaperones 2004;9:21-8.

53. Zoubeidi A, Zardan A, Beraldi E, et al. Cooperative interactions between androgen receptor (AR) and heat-shock protein 27 facilitate AR transcriptional activity. Cancer Res 2007;67:10455-65.

54. Matsumoto H, Yamamoto Y, Shiota M, et al. Cotargeting Androgen Receptor and Clusterin Delays Castrate-Resistant Prostate Cancer Progression by Inhibiting Adaptive Stress Response and AR Stability. Cancer Res 2013;73:5206-17.

55. Kiyama S, Morrison K, Zellweger T, et al. Castration-induced increases in insulin-like growth factor-binding protein 2 promotes proliferation of androgen-independent human prostate LNCaP tumors. Cancer Res 2003;63:3575-84.

56. Jeppsson F, Eketjäll S, Janson J, et al. Discovery of AZD3839, a Potent and Selective BACE1 Inhibitor Clinical Candidate for the Treatment of Alzheimer Disease. J Biol Chem. 2012 November 30; 287(49): 41245–41257.

57. Bubendorf L, Kolmer M, Kononen J, et al. Hormone therapy failure in human prostate cancer: analysis by complementary DNA and tissue microarrays. J Natl Cancer Inst 1999;91:1758-64.

58. Cornford PA, Dodson AR, Parsons KF, et al. Heat shock protein expression independently predicts clinical outcome in prostate cancer. Cancer Res 2000;60:7099-105.

59. Conroy SE, Sasieni PD, Amin V, et al. Antibodies to heat-shock protein 27 are associated with improved survival in patients with breast cancer. Br J Cancer 1998;77:1875-9.

60. Arts HJ, Hollema H, Lemstra W, et al. Heat-shock-protein-27 (hsp27) expression in ovarian carcinoma: relation in response to chemotherapy and prognosis. Int J Cancer 1999;84:234-8.

61. Zhang R, Tremblay TL, McDermid A, et al. Identification of differentially expressed proteins in human glioblastoma cell lines and tumors. Glia 2003;42:194-208.

62. Liu P, Cheng H, Roberts TM and Zhao JJ. Targeting the phosphoinositide 3-kinase pathway in cancer. Nat Rev Drug Discov 2009;8:627-44.

63. Paz-Ares L, Soulieres D, Melezinek I, et al. Clinical outcomes in non-small-cell lung cancer patients with EGFR mutations: pooled analysis. J Cell Mol Med 2010;14:51-69.

64. Bruey JM, Ducasse C, Bonniaud P, Ravagnan L, et al. Hsp27 negatively regulates cell death by interacting with cytochrome c. Nat Cell Biol 2000;2:645-52.

65. Pandey P, Farber R, Nakazawa A, et al. Hsp27 functions as a negative regulator of cytochrome c-dependent activation of procaspase-3. Oncogene 2000;19:1975-81.

66. Song H, Ethier SP, Dziubinski ML , et al. Stat3 modulates heat shock 27kDa protein expression in breast epithelial cells. Biochem Biophys Res Commun 2004;314:143-50.

67. Rocchi P, Jugpal P, So A, Sinneman S, et al. Small interference RNA targeting heat-shock protein 27 inhibits the growth of prostatic cell lines and induces apoptosis via caspase-3 activation in vitro. BJU Int 2006;98:1082-9.

68. Bausero MA, Page DT, Osinaga E et al. Surface expression of Hsp25 and Hsp72 differentially regulates tumor growth and metastasis. Tumour Biol 2004;25:243-51.

69. O'Callaghan-Sunol C, Gabai VL and Sherman MY. Hsp27 modulates p53 signaling and suppresses cellular senescence. Cancer Res 2007;67:11779-88.

70. Kang SH, Kang KW, Kim KH, et al. Upregulated HSP27 in human breast cancer cells reduces Herceptin susceptibility by increasing Her2 protein stability. BMC Cancer 2008;8:286.

71. McCollum AK, TenEyck CJ, Stensgard B, et al. P-Glycoprotein-mediated resistance to Hsp90-directed therapy is eclipsed by the heat shock response. Cancer Res 2008;68:7419-27.

72. Jovcevski B, Kelly MA, Rote AP, et al. Phosphomimics destabilize Hsp27 oligomeric assemblies and enhance chaperone activity. Chem Biol. 2015 Feb 19;22(2):186-95.

73. Musiani D, Konda JD, Pavan S, et al. Heat-shock protein 27 (HSP27, HSPB1) is up-regulated by MET kinase inhibitors and confers resistance to MET-targeted therapy. FASEB J 2014;28:4055-67.

LIST OF PUBLICATIONS: SUMMARY

1. Al Nakouzi N., Wang k C., Beraldi E., Jager W., Nappi L, Fazli L., Ettinger S., Bishop J., Zhang F., Chauchereau A., Loriot Y and Gleave M. Clusterin knockdown sensitizes prostate cancer cells to taxane by modulating mitosis. Submitted to EMBO Molecular Medicine.

Summary: Clusterin (CLU) is a stress-activated molecular chaperone involved in the treatment resistance to taxanes when highly expressed. Taxanes target cells in mitosis, a complex mechanism controlled in part by balancing antagonistic roles of Cdc25C and Wee1 in mitosis progression. This manuscript demonstrates that CLU silencing induces a constitutive activation of Cdc25C, which delays mitotic exit and hence sensitizes cancer cells to mitotic-targeting agents such taxanes. In this study we show that CLU silencing induces a constitutive activation of Cdc25C via the phosphatase PP2A leading to relief of negative feedback inhibition and activation of Wee1-Cdk1 to promote survival and limit therapeutic efficacy. Simultaneous inhibition of CLU-regulated cell cycle effector wee1, may improve synergistic responses of biologically rational combinatorial regimens using taxanes and CLU inhibitors.

2. Nappi L., Black P and Eigl B. Building the case for adjuvant chemotherapy after radical cystectomy. Accepted by Urology.

Summary: Neoadjuvant cisplatin-based chemotherapy is the optimal therapeutic option for eligible patients with muscle invasive bladder cancer. However, new studies support the use of adjuvant chemotherapy, using cisplatin based regimens, in patients with high risk tumors who did not receive neoadjuvant therapy.

3. Nappi L, Gleave ME. PARP inhibition in castration-resistant prostate cancer. Future Oncol. 2016 Jan 21.

Summary: DNA repair defects have been identified in many sporadic and hereditary prostate cancer tumors. Interestingly, the rate of the DNA-repair gene mutations increase during the

development of castration resistance disease. BRCA1 and BRCA2 are the most frequent DNA repair genes associated with prostate cancer development. The use of PARP-inhibitors demonstrated to significantly control tumor proliferation and increase survival of the patients affected by metastatic castration resistant prostate cancer harboring DNA-repair gene mutations.

4. Barbara Lelj-Garolla, Masafumi Kumano, Eliana Beraldi, Lucia Nappi, Palma Rocchi, Diana N. Ionescu, Ladan Fazli, Amina Zoubeidi, and Martin E. Gleave
Hsp27 inhibition with OGX-427 sensitizes non-small cell lung cancer cells to erlotinib and chemotherapy. Mol Cancer Ther. 2015 May;14(5):1107-16.

Summary: Hsp27 is a stress-induced chaperone that promotes acquired resistance in several cancers. This paper showed that Hsp27 is also involved in the resistance to EGFR targeted agents in NSCLC. Hsp27 inhibition, by OGX-427, a new generation Antisense Oligonucleotide in clinical phase of development, increases the sensitivity of NSCLC cells to EGFR inhibitors and chemotherapy.

5. Luigi Formisano#, Lucia Nappi#, Roberta Rosa, Roberta Marciano, Claudia D'Amato, Valentina D'Amato, Vincenzo Damiano, Lucia Raimondo, Francesca Iommelli, Antonella Scorziello, Giancarlo Troncone, Bianca Maria Veneziani, Sarah J Parsons, Sabino De Placido and Roberto Bianco.
Epidermal growth factor-receptor activation modulates Src-dependent resistance to lapatinib in breast cancer models. Breast Cancer Res. 2014 May 5;16(3):R45.

Summary: Src tyrosine kinase is involved in the resistance to human epidermal growth factor receptor 2 (HER2) inhibitors in breast cancer. This paper demonstrated that Src contributes to lapatinib resistance preferentially activating EGFR. Cotargeting of EGFR-HER2 synergistically inhibits survival, migration, and invasion of lapatinib resistant breast cancer cells, thereby counteracting Src-mediated resistance.

6. Claudia D'Amato, Roberta Rosa, Roberta Marciano, Valentina D'Amato, Luigi Formisano, Lucia Nappi, Lucia Raimondo, Concetta Di Mauro, Alberto Servetto, Marina Accardo, Chiara

Carlomagno, Cataldo Bianco, Fortunato Ciardiello, Bianca Maria Veneziani, Sabino De Placido and Roberto Bianco.
Inhibition of Hedgehog signaling by NVP-LDE225 (Erismodegib) interferes with growth and invasion of human renal cell carcinoma cells. Br J Cancer. 2014 Sep 9;111(6):1168-79.

Summary: Hedgehog (Hh) pathway contributes to the deveopment and progression of different human cancers. As demonstrated in this paper, inhibition of the Hh signaling represents a valid anticancer therapeutic approach also for renal cell carcinoma (RCC) patients. NVP-LDE225, a Smoothened (Smo) antagonist, cooperated with either everolimus or sunitinib to inhibit proliferation, migration, and invasion of RCC cells even in sunitinib-resistant (SuR) cells.

7. Valentina D'Amato, Roberta Rosa, Claudia D'Amato, Luigi Formisano, Lucia Nappi, Roberta Marciano, Lucia Raimondo, Concetta Di Mauro, Alberto Servetto, Celeste Fusciello, Bianca Maria Veneziani, Sabino De Placido and Roberto Bianco. The dual PI3K/mTOR inhibitor PKI-587 enhances sensitivity to the anti-EGFR monoclonal antibody cetuximab in human head and neck cancer models. Br J Cancer. 2014 Jun 10;110(12):2887-95.

Summary: Cetuximab, a monoclonal antibody against EGFR, is the only targeted agent approved for the treatment of head and neck squamous cell carcinomas (HNSCC). The phosphoinositide 3-kinase (PI3K) and the mammalian target of rapamycin (mTOR) pathways have an important role in the pathogenesis of HNSCC, and also in the development of the resistance to cetuximab, as demonstrated in this paper. The treatment with PKI-587, a PI3K inhibitor, sensitizes cells to cetuximab and overcomes EGFR inhibitor resistance.

8. Roberta Rosa, Roberta Marciano, Luigi Formisano, Lucia Nappi, Claudia D'Amato, Vincenzo Damiano, Gabriella Marfè, Silvana Del Vecchio, Antonella Zannetti, Adelaide Greco, Umberto Malapelle, Giancarlo Troncone, Alfonso De Stefano, Chiara Carlomagno, Bianca Maria Veneziani, Sabino De Placido, Roberto Bianco. Sphingosine Kinase 1 (SPHK1) overexpression contributes to cetuximab resistance in human colorectal cancer models. Clinical Cancer Research 2013 Jan 1;19(1):138-47.

Summary: Sphingosine kinase 1 (SphK1) is overactivated in colorectal cancer cells with intrinsic or acquired resistance to cetuximab. Moreover, as showed in this paper, a correlation between SphK1 expression and cetuximab response was found in colorectal cancer patients. SphK1 inhibition by N,N-dimethyl-sphingosine or silencing via siRNA in resistant cells restores sensitivity to cetuximab, whereas exogenous SphK1 overexpression in sensitive cells confers resistance to these agents. In addition, treatment of resistant cells with fingolimod (FTY720), a S1P receptor (S1PR) antagonist, resulted in resensitization to cetuximab.

9. Roberta Rosa, Vincenzo Damiano, Lucia Nappi, Luigi Formisano, Francesco Massari, Aldo Scarpa, Guido Martignoni, Roberto Bianco, Giampaolo Tortora. Angiogenic and signalling proteins affect resistance and choice of second line treatment in renal cell cancer. Br J Cancer. 2013 Aug 6;109(3):686-93.

Summary: The effect of sunitinib, sorafenib and everolimus, multi-TK inhibitors approved for the treatment of metastatic renal cell carcinoma, alone and in sequence, was assessed in a vitro and in vivo in a panel of human RCC cells. As single agents, sunitinib, sorafenib and everolimus share similar activity in inhibiting cell proliferation, signal transduction and vascular endothelial growth factor (VEGF) secretion. Pre-treatment with sunitinib reduced the response to subsequent sunitinib and sorafenib but not to everolimus. Inability by sunitinib to persistently inhibit HIF-1, VEGF and pMAPK anticipated treatment resistance in xenografted tumours. After first-line sunitinib, second-line treatment with everolimus was more effective than either sorafenib or rechallenge with sunitinib in interfering with signalling proteins, VEGF and interleukin-8, translating into a significant advantage in tumour growth inhibition and mice survival.

10. Damiano V, Rosa R, Formisano L, Nappi L, Gelardi T, Marciano R, Cozzolino I, Troncone G, Agrawal S, Veneziani BM, De Placido S, Bianco R, Tortora G.
Toll-like receptor 9 agonist IMO cooperates with everolimus in renal cell carcinoma by interfering with tumour growth and angiogenesis. Br J Cancer. 2013 Apr 30;108(8):1616-23.

Summary: The Toll-like receptor 9 agonist immune modulatory oligonucleotide (IMO) exhibits direct antitumour and antiangiogenic activity and cooperates with both epidermal growth factor

receptor (EGFR) and vascular endothelial growth factor (VEGF) inhibitors. The combination of IMO and everolimus synergistically inhibited in vitro growth and survival of RCC cell lines. Moreover, everolimus plus IMO interfered with EGFR-dependent signaling and reduced VEGF secretion in both VHL wild-type and mutant cells. A combined treatment with everolimus and IMO is effective in VHL wild-type and mutant models of RCC by interfering with tumour growth and angiogenesis, thus representing a potentially effective, rationale-based combination to be translated in the clinical setting.

11. Monteleone F, Rosa R, Vitale M, D'Ambrosio C, Succoio M, Formisano L, Nappi L, Romano MF, Scaloni A, Tortora G, Bianco R, Zambrano N.
Increased anaerobic metabolism is a distinctive signature in a colorectal cancer cellular model of resistance to antiepidermal growth factor receptor antibody. Proteomics. 2013 Mar;13(5):866-77.

Summary: The protein expression profile between cetuximab-sensitive and -resistant colorectal cancer cells was assessed in this paper. Combined 2D DIGE and MS analyses revealed specific proteomic signature of various metabolic enzymes: glucose-6-phosphate dehydrogenase, transketolase, lactate dehydrogenase B, and pyruvate dehydrogenase E1. Resistant cells also showed decreased nicotinamide adenine dinucleotide phosphate (NADPH) levels. These data demonstrate that increased anaerobic metabolism is a prominent feature observed in the colorectal cells with acquired resistance to anti-EGFR drug cetuximab.